Molecular Dihydrogen and Hydrido Derivatives of Ruthenium(II) Complexes Containing Chelating Ferrocenyl-Based Tertiary Phosphine Amine Ligands and/or Monodentate Tertiary Phosphine Ligands

Cashman R. S. M. Hampton,[1a] Ian R. Butler,[1a] William R. Cullen,*[,1a] Brian R. James,*[,1a] Jean-Pierre Charland,[1b] and J. Simpson[1c]

Departments of Chemistry, University of British Columbia, Vancouver, Canada V6T 1Z1, and University of Otago, P.O. Box 56, Dunedin, New Zealand, and Division of Chemistry, National Research Council, Ottawa, Ontario, Canada K1A 0R6

Received October 15, 1991

Reactions of complexes of the type $RuCl_2(PPh_3)$(P-N) with H_2 are reported, where P-N represents the chelating ferrocene-based ligands (η-C_5H_5)Fe(η-C_5H_3(CHMeNMe$_2$)PR$_2$-1,2) with R = *i*-Pr (the isoPFA ligand) or Ph (the PPFA ligand). Depending on the solvent(s) used, and absence or presence of added base, $RuCl_2(PPh_3)$(isoPFA) (**2b**) generates the dinuclear η^2-H_2 complexes $L_2(\eta^2\text{-}H_2)Ru(\mu\text{-}Cl)_2(\mu\text{-}H)Ru(H)(PPh_3)_2$ where L_2 = isoPFA (complex **3**) or $L_2 = (PPh_3)_2$ (complex **4**). *n*-Butanol solutions of $RuCl_2(PPh_3)$(PPFA) (**2a**) under H_2 also yield **4**, as well as $Ru(H)Cl_2(PPh_3)$(PPFA·H)(BuOH), a zwitterionic species containing a protonated amine moiety stabilized by coordinated *n*-BuOH, which is a likely intermediate in heterolytic cleavage of the H_2: the complex RuH(Cl)-(PPh_3)(isoPFA) (**5**), together with a hydrido carbonyl species, is isolated from methanol solutions of **2b**. Complexes **2b**, **3**, **4**, and **5** are characterized by X-ray crystallography; the mononuclear complexes **2b** and **5** are orthorhombic with space groups *F*2*dd* and $P2_12_12_1$, respectively. For **2b**, a = 10.4316 (3) Å, b = 31.4693 (10) Å, c = 43.2963 (18) Å, V = 14213.1 (8) Å^3, and Z = 16; the structure refined to R = 0.054 and R_w = 0.046 for 1783 reflections with $I > 2\sigma(I)$. Corresponding crystallographic data for **5** are a = 9.915 (2) Å, b = 16.511 (4) Å, c = 21.781 (5) Å, V = 3566 (1) Å^3, Z = 4, R = 0.077, and R_w = 0.079 for 2691 reflections. The essential crystallographic data for the dinuclear complex **3** have been published [Hampton, C.; et al. *J. Am. Chem. Soc.* **1988**, *110*, 6918]. The related complex **4** crystallizes in the monoclinic system, space group $P2_1/c$, with a = 15.866 (5) Å, b = 18.931 (5) Å, c = 24.472 (7) Å, β = 108.69 (2)°, V = 6963 (3) Å^3, Z = 4, R = 0.078, and R_w = 0.0792 for 4507 reflections. Variable-temperature ^{1}H- and ^{31}P-NMR data for **3** reveal fast exchange between the η^2-H_2 and the μ-H at 20 °C and a slower exchange of this system with the terminal hydride; corresponding data for **4** and its P(*p*-tolyl)$_3$ analogue **7** show a faster exchange involving all the hydrogens. Activation parameters are determined for the exchange processes.

Introduction

The ferrocene-based ligands **1** are phosphines that contain a chelating soft/hard P–N donor assembly that has both planar and central elements of chirality.[2] Metal complexes of these ligands have been studied extensively as homogeneous catalysts for hydrogenation and hydrosilylation of olefins and ketones, hydroformylation of olefins, allylic amination, and cross-coupling reactions between organometallic compounds and alkyl/aryl halides, including enantioselective syntheses.[3]

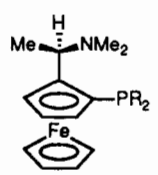

1: PPFA (R = Ph) and isoPFA (R = *i*-Pr)

Our original interest in ruthenium derivatives of **1**[4] was to evaluate the catalytic activity of $RuCl_2(PPh_3)$(PPFA) with respect to that of the well-known complex $RuCl_2(PPh_3)_3$. The new complex proved to be an active catalyst for the hydrogenation of 1-hexene, and because hydrides were not originally detected when the catalyst was exposed to hydrogen, even though a reaction did occur, a suggestion was made that the mechanism for the catalytic reaction was based on the initial reduction of the Ru(II) to Ru(I).[4]

The present paper describes a continuation of our studies on the reaction of hydrogen with $RuCl_2(PPh_3)$(PPFA) (**2a**) and an extension of the work to $RuCl_2(PPh_3)$(isoPFA) (**2b**). We report the structures of **2b** and $(\eta^2\text{-}H_2)$(isoPFA)$Ru(\mu\text{-}Cl)_2(\mu\text{-}H)RuH(PPh_3)_2$ (**3**), which is obtained from **2b** by reaction with dihydrogen.[5] The structure of one other such reaction product, Ru(H)(Cl)(PPh_3)(isoPFA) (**5**), is described, as are NMR spectroscopic studies on exchange processes involving the η^2-H_2 ligand in **3** and the related molecules $(\eta^2\text{-}H_2)(PAr_3)_2Ru(\mu\text{-}Cl)_2(\mu\text{-}H)RuH(PAr_3)_2$ (**4**, Ar = Ph; **7**, Ar = *p*-tolyl). Some structural data on **4** are also presented, although the metal-bound H atoms were not located.

Experimental Section

Air-sensitive materials were manipulated in a nitrogen or hydrogen atmosphere by using Schlenk techniques. THF was dried by using sodium/

(1) (a) University of British Columbia. (b) National Research Council. (c) University of Otago.
(2) Battelle, L. F.; Bau, R.; Gokel, G. W.; Oyakawa, R. T.; Ugi, I. K. *J. Am. Chem. Soc.* **1973**, *95*, 482.
(3) (a) Cullen, W. R.; Woollins, J. D. *Coord. Chem. Rev.* **1981**, *39*, 1. (b) Hayashi, T.; Kumada, M. *Acc. Chem. Res.* **1982**, *15*, 359. (c) Cullen, W. R.; Han, N. F. *J. Organomet. Chem.* **1987**, *333*, 269. (d) Hayashi, T.; Yamamoto, A.; Ito, Y.; Nishioka, E.; Miura, H.; Yanagi, K. *J. Am. Chem. Soc.* **1989**, *111*, 6301.
(4) Rodgers, G. E.; Cullen, W. R.; James, B. R. *Can. J. Chem.* **1983**, *61*, 1314. The ^{31}P{^{1}H}-NMR data for **2a** were given incorrectly in this paper; the correct data are (121 MHz, C_6D_6, ambient temperature) δ 77.5(d), 44.3(d), $^2J_{PP}$ = 39 Hz.
(5) For a preliminary communication see Hampton, C.; Cullen, W. R.; James, B. R.; Charland, J.-P. *J. Am. Chem. Soc.* **1988**, *110*, 6918.

0020-1669/92/1331-5509$03.00/0

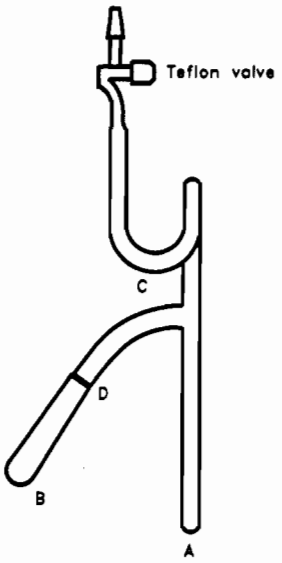

Figure 1. Glass apparatus used for manipulating materials under hydrogen (0–10 atm). The diagram is approximately to scale, and the height is ~40 cm.

benzophenone; diethyl ether, hexane, benzene, and *N*,*N*-dimethylacetamide (DMA) were dried by using CaH_2; alcohols were dried by using Mg/I_2. The following spectrometers were used: Bruker WP80, WH400, and Varian XL 300 for NMR; Perkin-Elmer 552A for UV/vis; Nicolet 5DX for FTIR. The program DNMR4 (Quantum Chemistry Program Exchange, Department of Chemistry, University of Indiana), adapted for local use, was employed to simulate chemical-exchange NMR spectra. $^{31}P\{^1H\}$ signals are reported relative to 85% aqueous H_3PO_4, downfield shifts being positive. For NMR signals, s = singlet, d = doublet, t = triplet, q = quartet, m = multiplet, and br = broad.

Preparation of Dichloro{1-[α-(dimethylamino)ethyl]-2-(diisopropylphosphino)ferrocene}(triphenylphosphine)ruthenium(II), $RuCl_2(PPh_3)$-(isoPFA) (2b). $RuCl_2(PPh_3)_3$ (0.8 g, 0.8 mmol)[6] and racemic isoPFA (0.56 g, 1.5 mmol)[7] were refluxed overnight under nitrogen in a solvent mixture of hexane (50 mL) and $CHCl_3$ (5 mL). The suspended $RuCl_2$-$(PPh_3)_3$ gradually reacted to give a green, sparingly soluble product that was isolated by filtration and washed with hexane. The solid was dissolved in hot benzene, the solution was filtered, and the volume was reduced to 10 mL. Hexane (50 mL) was then layered onto this solution under nitrogen, and crystallization allowed to occur slowly at −30 °C over several days. The dark-green product was isolated by filtration and washed with hexane. Yield: 67%. Alternatively, recrystallization from CH_2Cl_2/hexane of the initially precipitated crude product, followed by a second recrystallization from THF, resulted in a pure product. $^{31}P\{^1H\}$ NMR (121 MHz, $CDCl_3$): δ 96.2 (d), 36.6 (d), $^2J_{PP}$ = 32 Hz. ^1H NMR (300 MHz, $CDCl_3$): δ 0.72 (m, 6H, PCHCH_3), 1.18 (dd, 3H, $^3J_{PH}$ = 15 Hz, $^3J_{HH}$ = 7 Hz, PCHCH_3), 1.43 (d, 3H, $^3J_{HH}$ = 7 Hz, FcCHCH_3), 1.75 (dd, 3H, $^3J_{PH}$ = 13 Hz, $^3J_{HH}$ = 7 Hz, PCHCH_3), 2.24, 2.82 (2m, 2H, PCHCH$_3$), 2.35, 2.44 (2s, 6H, N(CH_3)$_2$), 4.22 (s, 5H, FeC_5H_5), 4.4 (t, 1H, J_{HH} = 3 Hz, FeC_5H_3), 4.58 (bs, 2H, FeC_5H_3), 6.2 (q, 1H, $^3J_{HH}$ = 6 Hz, FcCHCH$_3$), 7.37 (m, 9H, Ph meta, para), 7.92 (t, 6H, J = 8 Hz, Ph ortho). Anal. Calcd for $C_{38}H_{47}Cl_2FeNP_2Ru$: C, 56.52; H, 5.82; N, 1.73. Found: C, 56.30; H, 6.06; N, 1.68.

Preparation of Bis(μ-chloro)(μ-hydrido)(η²-dihydrogen)(hydrido)bis-(triphenylphosphine){1-[α-(dimethylamino)ethyl]-2-(diisopropylphosphino)-ferrocene}diruthenium(II), $(\eta^2\text{-}H_2)$(isoPFA)Ru(μ-Cl)$_2$(μ-H)RuH$(PPh_3)_2$ (3). All manipulations were carried out under a hydrogen atmosphere and in the apparatus shown in Figure 1. Complex **2b** was added with a small spin bar via the Teflon valve, and shaken down to A; solvent was vacuum-transferred into C, and after evacuation (with the solvent frozen) H_2 was added prior to warming the apparatus and mixing the reagents in A. Cooling at B allows the use of frit D for isolating and washing solid products, and section A could be used subsequently for recrystallization. A suspension of complex **2b** (0.334 g, 0.41 mmol) in a benzene/methanol (10:1) solvent mixture (4 mL) was reacted with H_2 (1–4 atm) at room temperature. Reaction occurred in 4–10 days to give a brown solution and an orange precipitate. Because of the solubility limitation, larger quantities of the reagents required longer reaction times. The reaction rate also appeared to depend on the methanol concentration. The precipitate was isolated and washed with methanol and benzene. Yield: 0.094 g (39%). $^{31}P\{^1H\}$ NMR (121 MHz, CD_2Cl_2, 20 °C, 2–3 atm of hydrogen): δ 78.6, 78.4 (two overlapping doublets with $^2J_{PP}$ 40 Hz, PPh_3 trans to Cl), 77.2 (br s or possibly two br s overlapping, isoPFA), 64.7, 64.5 (two overlapping doublets with $^2J_{PP}$ = 40 Hz, PPh_3 trans to μ-H). ^1H NMR (300 MHz, CD_2Cl_2, 20 °C, 2–3 atm of hydrogen): δ −18.6 (dd, $^2J_{PH}$ = 28, 32 Hz, Ru–H), −12 to −17 (br s, η^2-H_2 and μ-H exchanging), 0.3, 0.39, 1.5, 1.8 (4dd, 12H, $^3J_{PH}$ = 15 Hz, $^3J_{HH}$ = 7 Hz, PCHCH_3), 1.48 (d, 3H, $^3J_{HH}$ = 7 Hz, FcCHCH_3), 2.35, 3.1 (2s, 6H, N(CH_3)$_2$), 4.1 (s, 5H, C_5H_5), 4.08, 4.35, 4.45 (3s, 3H, C_5H_3), 4.45 (q, 1H, $^3J_{HH}$ = 7 Hz, FcCHCH$_3$) (the signal at 4.45 is better resolved in $CDCl_3$), 6.9–7.2 (m, 18H, Ph meta, para), 7.4, 7.55 (2t, 12H, J_{HH} = 9 Hz, Ph ortho). IR (KBr): 2109, 2025 cm^{-1}. Anal. Calcd for $C_{56}H_{66}Cl_2FeNP_3Ru_2$: C, 57.24; H, 5.67; N, 1.19. Found: C, 57.37; H, 6.02; N, 1.39.

Crystals of **3**·1.5C_6H_6 were obtained by layering hexane onto a benzene/dichloromethane (9:5) solution of **3**.

Other crystals (some white, some black-red, the latter being diamond shaped) gradually grew in the benzene/methanol/dichloromethane/hexane filtrate/wash solution, under hydrogen in section B of the reaction vessel. These crystals were filtered off at the frit by inverting the tube and applying a pressure differential across the frit and then washed with hexane. The white crystalline material was identified as dimethylammonium chloride on the basis of its ^1H NMR and mass spectra. The black-red crystals are those of an unidentified ruthenium hydride.

Reaction of $RuCl_2(PPh_3)$(isoPFA) with H_2 in DMA/C_6D_6. The complex **2b** (0.032 g, 0.040 mmol) was stirred under H_2 (7 atm) in a solvent mixture of DMA/C_6D_6 1:1 (2 mL) at ambient temperature for 6 h, and the solution then transferred under H_2 to an NMR tube that was subsequently sealed. No precipitate was observed. The $^{31}P\{H\}$ NMR spectrum showed the presence of the following species: (i) unreacted **2b**, identified by two doublets at δ 35.7 and 94.7 with $^2J_{PP}$ = 32 Hz; (ii) $(\eta^2\text{-}H_2)$(isoPFA)Ru(μ-Cl)$_2$(μ-H)RuH$(PPh_3)_2$ (**3**), identified by resonances at δ 78.6 (dd), 76.8 (s), 64.5 (dd); (iii) $(\eta^2\text{-}H_2)(PPh_3)_2$Ru(μ-Cl)$_2$(μ-H)RuH$(PPh_3)_2$ (**4**), identified by the two broad singlets at δ 70.3 and 46.0;[8] (iv) an unidentified species with a broad singlet at δ −13.9. Also observed were the following. (vi) RuH(Cl)(PPh_3)(isoPFA) (**5**) (see below), identified by two doublets at δ 98.0 and 61.0; (vii) Ru(H)Cl-$(PPh_3)_3$, the singlet at δ 59.3 is close to that reported for the CH_2Cl_2 solution of this complex (δ 59.0).[9] Several unidentified minor resonances were also seen.

Reaction of $RuCl_2(PPh_3)$(isoPFA) with H_2 in DMA. (a) $RuCl_2(PPh_3)$-(isoPFA) (0.45 g, 0.56 mmol) was stirred in DMA (3 mL) under hydrogen (10 atm) for 4 days at ambient temperature. An orange precipitate formed. The reaction mixture was filtered under hydrogen and the solid washed twice with methanol and once with hexane. The product was identified as $(\eta^2\text{-}H_2)(PPh_3)_2$Ru(μ-H)(μ-Cl)$_2RuH(PPh_3)_2$·2DMA (**4**·2DMA). The yield was estimated to be ~70 mg (~40%). The $^{31}P\{^1H\}$ and ^1H NMR spectra were the same as reported previously, as well as for the known DMA-free complex.[8,10] IR: 2129, 1970, 1903, 1822 cm^{-1}, all broad, weak. Anal. Calcd for $C_{80}H_{82}Cl_2N_2O_2P_4Ru_2$: C, 64.04; H, 5.51; N, 1.87. Found: C, 63.75; H, 5.43; N, 1.64.

(b) Complex **2b** (0.2 g, 0.25 mmol) and PPh_3 (1.3 g, 5 mmol) were stirred in 5 mL of DMA under 1 atm of H_2 for 2 days at ambient temperature in a standard Schlenk apparatus. The resulting violet precipitate was washed three times with hexane, dried, and identified as Ru(H)Cl$(PPh_3)_3$. ^1H NMR (80 MHz, $CDCl_3$): δ −17.4 (q, $^2J_{PH}$ = 25 Hz, Ru–H).[11] The yield was 90%.

Preparation of Chloro(hydrido){1-[α-(dimethylamino)ethyl]-2-(diisopropylphosphino)ferrocene}(triphenylphosphine)ruthenium(II), RuH(Cl)-(PPh_3)(isoPFA) (5). The complex **2b** (0.08 g, 0.1 mmol) and Proton Sponge (1,8-bis(dimethylamino)naphthalene) (0.023 g, 0.1 mmol) were placed under nitrogen in methanol (1–2 mL) for 5 months. Large deep-

(6) Stephenson, T. A.; Wilkinson, G. *J. Inorg. Nucl. Chem.* **1966**, *28*, 945.
(7) Butler, I. R.; Cullen, W. R.; Kim, T.-J. *Synth. React. Inorg. Met.-Org. Chem.* **1985**, *15*, 109.
(8) (a) Dekleva, T. W. Ph.D. Thesis, University of British Columbia, Vancouver, 1983. (b) Dekleva, T. W.; Thorburn, I. S.; James, B. R. *Inorg. Chim. Acta* **1985**, *100*, 49.
(9) Hoffman, P. R.; Caulton, K. G. *J. Am. Chem. Soc.* **1975**, *97*, 4221.
(10) Hampton, C.; Dekleva, T. W.; James, B. R.; Cullen, W. R. *Inorg. Chim. Acta* **1988**, *145*, 165.
(11) For Ru(H)Cl$(PPh_3)_3$: δ_{CDCl_3} (25 °C) −17.44 (q, $^2J_{PH}$ = 26 Hz);[12] δ_{CDCl_3} (30 °C) −17.78 (q, $^2J_{PH}$ = 26 Hz).[8]
(12) Hallman, P. S.; McGarvey, B. R.; Wilkinson, G. *J. Chem. Soc. A* **1968**, 3143.

Table I. Crystal Data for **2b** and **5**

	2b	**5**
formula	$C_{38}H_{47}Cl_2FeNP_2Ru$	$C_{38}H_{48}ClFeNP_2Ru$
fw	807.57	773.12
T, °C	20	−100
cryst syst	orthorhombic	orthorhombic
Z	16	4
space group	*F2dd*	$P2_12_12_1$ (No. 19)
a, Å	10.4316 (3)	9.915 (2)
b, Å	31.4693 (10)	16.511 (4)
c, Å	43.2963 (18)	21.781 (5)
V, Å^3	14213.1 (8)	3566 (1)
μ, mm^{-1}	1.09	1.02
λ, Å	0.710 69 (Mo Kα)	0.710 69 (Mo Kα)
R(sign reflcns)[a]	0.056	0.077
R_w(sign reflcns)[b]	0.048	0.079
resid density, e/Å^3	<0.59	<0.48

[a] $R = \sum||F_o| - |F_c||/\sum|F_o|$. [b] $R_w = (\sum w(|F_o| - |F_c|)^2/\sum w|F_o|^2)^{1/2}$.

red crystals (~20 mg) of **5** grew in this time, as well as yellow crystals of $RuH(Cl)(CO)(PPh_3)$(isoPFA) (**6**).[13] This mixture of crystals was separated from the solution by filtration, washed with methanol, and dried. The crystals of **5** were then isolated by hand-picking. $^{31}P\{^1H\}$ NMR ($CDCl_3$, 121 MHz): δ 98.0 (d), 61.5 (d), $^2J_{PP}$ = 40 Hz. ^1H NMR ($CDCl_3$, 300 MHz): δ −23.1 (dd, $^2J_{PH}$ = 40, 27 Hz, Ru*H*). IR: 2028 cm^{-1} (w) ν(RuH). Anal. Calcd for $C_{38}H_{48}ClFeNP_2Ru$: C, 59.06; H, 6.22; N, 1.81. Found: C, 58.38; H, 6.00; N, 1.80.

Preparation of Bis(μ-chloro)(μ-hydrido)(η^2-dihydrogen)(hydrido)-tetrakis(triarylphosphine)diruthenium(II), $Ru_2(\eta^2\text{-}H_2)H_2Cl_2(PR_3)_4$ (R = phenyl (4), *p*-tolyl (7)). The DMA-free title complexes were prepared as described elsewhere[8] from $[RuCl_2(PPh_3)_2]_2$ and 1 atm of H_2 in toluene in the presence of Proton Sponge and from $RuCl_3(P(p\text{-tolyl})_3)_2$(DMA) and 1 atm of H_2 in benzene in the presence of Proton Sponge, respectively. (**4**): $^{31}P\{^1H\}$ NMR (121 MHz, toluene-d_8, 20 °C, hydrogen atmosphere) δ 70.5, 46.0 (lit.[8] δ 68.0, 43.1). Anal. Calcd for $C_{72}H_{64}Cl_2P_4Ru_2$: C, 65.19; H, 4.87. Found: C, 64.95; H, 4.93.

7: $^{31}P\{^1H\}$ NMR (121 MHz, CD_2Cl_2, 20 °C, 2–3 atm of hydrogen) δ 68.8, 44.7 (lit.[8] 69.2, 44.0).

Further information on the $^{31}P\{^1H\}$ and the ^1H NMR spectra of **4** and **7** is presented below.

Reactions of $RuCl_2(PPh_3)$(PPFA) (2a) with H_2 in Butanol. The complex **2a**,[4] (0.5 g, 0.6 mmol) was reacted with 2–8 atm of H_2 overnight in dry *n*-butanol (3 mL); **2a** was largely undissolved initially, but the suspension gradually changed to give a brown solution and yellow crystalline precipitate. The yellow solid was collected, washed with butanol, and then very small quantities of toluene (e.g., 3 × 0.2 mL). The NMR spectra of this solid in CD_2Cl_2 under an H_2 atmosphere showed the presence of unreacted **2a** and **4**, in addition to a major component **8**. $^{31}P\{^1H\}$ NMR (121 MHz, 20 °C): δ 71.11 (d, $^2J_{PP}$ = 40 Hz), 70.97 (d, $^2J_{PP}$ = 43 Hz), 64.72 (d, $^2J_{PP}$ = 40 Hz), 64.59 (d, $^2J_{PP}$ = 43 Hz). ^1H NMR (300 MHz, 20 °C): δ −20.4 (t, $^2J_{PH}$ = 32 Hz).

Anal. Calcd for $C_{48}H_{55}Cl_2FeNOP_2Ru$ [Ru(H)Cl_2(PPh_3)-(PPFA·H)BuOH]: C, 60.57; H, 5.83; Cl, 7.46; N, 1.47. Found: C, 59.37; H, 5.93; Cl, 9.50; N, 1.30.

X-ray Data Collection and Reduction for $RuCl_2(PPh_3)$(isoPFA) (2b). A single black-green crystal of **2b** was hand-picked and mounted on a glass fiber for cell-parameter determination and diffracted-intensity measurement. A Nonius CAD-4 diffractometer using graphite-monochromated Mo Kα radiation was employed to collect room-temperature diffraction data. Accurate cell parameters were measured from high-angle reflections. Some crystal data are provided in Table I.

The space group *F2dd* was uniquely defined from the systematic absences noted in the data set. The data were corrected in the usual fashion for Lorentz and polarization-ratio factors, but not for absorption. Other details pertaining to the data-reduction step are listed in Table I.

The positions of the heaviest non-hydrogen atoms, namely Fe, Ru, P, and Cl, were located using the direct methods structure solution program MULTAN.[14a] At this stage, isotropic refinement of all non-H atoms was carried out by full-matrix least-squares methods. A subsequent *D*-map revealed the position of the lighter non-H atoms and isotropic refinement was resumed. Next, H atoms were inserted at calculated positions, assuming sp^2 or sp^3 geometry where appropriate. They were included but not refined. Non-H atoms were refined anisotropically. PPh_3 phenyls were refined as rigid groups. The structures were refined to convergency by full-matrix least-squares. $\sum w(|F_o| - |F_c|)^2$ was minimized with $w^{-1} = \sigma^2(F_o) + 0.0003(F_o)^2$. The chirality parameter ETA was refined (0.9 (2)) to ensure that the correct enantiomorph was used in the refinement.[14b] Details of the structure refinement and final *D*-maps are given in Table I.

Table II. Atomic Parameters x, y, z, and B_{iso} for Non-Hydrogen Atoms of $RuCl_2(PPh_3)$(isoPFA) (**2b**)

atom	x	y	z	B_{iso},[a] Å^2
Ru	0.40689	0.13633 (4)	0.76573 (3)	1.97 (6)
Fe	0.7872 (4)	0.15011 (9)	0.69926 (6)	2.84 (13)
Cl(1)	0.5322 (6)	0.19840 (12)	0.77508 (9)	2.81 (21)
Cl(2)	0.2343 (6)	0.08740 (17)	0.75694 (11)	3.49 (24)
P(1)	0.5781 (6)	0.09719 (16)	0.75626 (11)	2.25 (22)
P(2)	0.3668 (5)	0.13009 (14)	0.81821 (10)	2.43 (24)
N	0.3744 (13)	0.1590 (4)	0.7165 (3)	1.9 (7)
C(1)	0.6406 (14)	0.1136 (4)	0.71804 (18)	2.6 (8)
C(2)	0.5870 (12)	0.1419 (3)	0.6961 (3)	2.4 (9)
C(3)	0.6482 (13)	0.1341 (4)	0.66747 (21)	2.7 (8)
C(4)	0.7384 (12)	0.1016 (4)	0.67134 (24)	2.8 (9)
C(5)	0.7434 (13)	0.0863 (4)	0.7010 (3)	3.1 (9)
C(6)	0.8079 (13)	0.2130 (4)	0.7099 (4)	4.7 (11)
C(7)	0.8651 (17)	0.2028 (5)	0.6811 (3)	3.7 (10)
C(8)	0.9574 (15)	0.1712 (5)	0.6857 (4)	4.5 (12)
C(9)	0.9678 (15)	0.1587 (5)	0.7160 (5)	5.3 (14)
C(10)	0.8663 (17)	0.1870 (6)	0.73259 (25)	5.3 (12)
C(11)	0.4961 (17)	0.1776 (5)	0.7030 (4)	2.1 (8)
C(12)	0.4755 (21)	0.2062 (7)	0.6741 (4)	4.4 (10)
C(13)	0.3166 (18)	0.1292 (5)	0.6944 (3)	2.5 (8)
C(14)	0.2818 (21)	0.1931 (6)	0.7232 (4)	3.5 (9)
C(15)	0.5551 (20)	0.0385 (4)	0.7488 (4)	2.8 (9)
C(16)	0.4893 (21)	0.0278 (5)	0.7203 (4)	3.6 (10)
C(17)	0.4916 (20)	0.0153 (5)	0.7762 (4)	3.6 (9)
C(18)	0.7134 (19)	0.1013 (5)	0.7833 (3)	2.6 (8)
C(19)	0.8437 (20)	0.0835 (6)	0.7716 (4)	3.8 (10)
C(20)	0.6893 (18)	0.0816 (5)	0.8145 (4)	3.7 (10)
C(21)	0.1899 (12)	0.1917 (4)	0.80242 (25)	3.3 (9)
C(22)	0.0685 (14)	0.2099 (3)	0.7998 (3)	3.8 (10)
C(23)	−0.0363 (11)	0.1911 (4)	0.8145 (3)	3.7 (10)
C(24)	−0.0196 (11)	0.1541 (4)	0.8317 (3)	3.6 (10)
C(25)	0.1019 (14)	0.1358 (3)	0.83434 (25)	3.1 (10)
C(26)	0.2066 (10)	0.1546 (4)	0.8197 (3)	3.0 (9)
C(27)	0.3451 (13)	0.0788 (3)	0.83881 (23)	3.0 (9)
C(28)	0.2534 (12)	0.0495 (4)	0.82914 (23)	3.1 (9)
C(29)	0.2426 (12)	0.0104 (3)	0.8441 (3)	3.6 (10)
C(30)	0.3234 (15)	0.0007 (3)	0.8688 (3)	3.6 (10)
C(31)	0.4152 (13)	0.0301 (4)	0.87849 (21)	3.5 (9)
C(32)	0.4260 (12)	0.0692 (3)	0.86348 (24)	2.6 (8)
C(33)	0.4484 (14)	0.1635 (3)	0.84793 (21)	3.3 (11)
C(34)	0.3760 (12)	0.1782 (4)	0.8728 (3)	4.0 (10)
C(35)	0.4335 (17)	0.2031 (4)	0.89561 (22)	6.0 (13)
C(36)	0.5633 (18)	0.2133 (3)	0.8935 (3)	5.2 (14)
C(37)	0.6357 (13)	0.1986 (4)	0.8686 (3)	4.9 (12)
C(38)	0.5783 (14)	0.1737 (4)	0.84583 (24)	3.4 (9)

[a] B_{iso} is the mean of the principle axes of the thermal ellipsoid.

All computations were performed with the NRCVAX crystal structure package.[15] The scattering curves were from ref 16. Table II lists the refined coordinates and equivalent isotropic thermal parameters of the non-H atoms, while selected bond lengths and angles involving such atoms are presented in Table III. Complete crystal data, lists of anisotropic temperature factors, H-atom parameters, and all bond lengths and angles, are deposited as Supplementary Material (Tables SI–SIV).

X-ray Data Collection and Resolution for 3. This structure was determined by using the same procedure as outlined above for **2b**. Relevant crystal data and details of analysis are listed in ref 5. Final positional and isotropic thermal parameters are given in Table IV, and bond lengths and angles of Ru-bonded atoms are listed in Table V. Supplementary material has already been deposited.[5]

(13) The structure and chemistry of **6** will be discussed in future publications from these laboratories.

(14) (a) Germain, G.; Main, P.; Woolfson, M. M. *Acta Crystallogr.* **1971**, *A27*, 368. (b) Rogers, D. *Acta Crystallogr.* **1981**, *A37*, 734.

(15) Gabe, E. J.; Le Page, Y.; Charland, J.-P.; Lee, F. L.; White, P. S. NRCVAX—an interactive program system for structure analysis. *J. Appl. Crystallogr.* **1989**, *22*, 384.

(16) *International Tables for X-ray Crystallography*; Birmingham: Kynoch Press: Birmingham, England, 1974; Vol. 4 (present distributor: Kluwer Academic Publishers, Dordrecht, The Netherlands).

Table III. Selected Bond Lengths (Å) and Angles (deg) for $RuCl_2(PPh_3)$(isoPFA) (**2b**)

Ru–Cl(1)	2.385 (5)	N–C(11)	1.515 (21)	Fe–C(8)	1.985 (16)	C(3)–C(2)	1.417 (16)
Ru–Cl(2)	2.399 (6)	N–C(13)	1.469 (21)	Fe–C(9)	2.037 (17)	C(4)–C(5)	1.371 (17)
Ru–P(1)	2.208 (6)	N–C(14)	1.472 (25)	Fe–C(10)	2.028 (15)	C(5)–C(1)	1.560 (18)
Ru–P(2)	2.319 (4)	C(11)–C(12)	1.557 (25)	Fe–C(6)	2.042 (14)	C(1)–C(2)	1.416 (17)
Ru–N	2.273 (12)	C(11)–C(2)	1.500 (21)	P(1)–C(15)	1.891 (15)	C(7)–C(8)	1.400 (23)
Fe–C(3)	2.061 (12)	C(15)–C(16)	1.45 (3)	P(1)–C(18)	1.838 (19)	C(7)–C(6)	1.417 (21)
Fe–C(4)	2.013 (12)	C(15)–C(17)	1.541 (24)	P(1)–C(1)	1.853 (11)	C(8)–C(9)	1.37 (3)
Fe–C(5)	2.059 (12)	C(18)–C(19)	1.56 (3)	P(2)–C(26)	1.842 (12)	C(9)–C(10)	1.560 (24)
Fe–C(1)	2.077 (14)	C(18)–C(20)	1.508 (23)	P(2)–C(27)	1.857 (10)	C(10)–C(6)	1.416 (22)
Fe–C(2)	2.108 (13)	C(26)–C(21)[a]	1.395 (16)	P(2)–C(33)	1.867 (12)		
Fe–C(7)	2.008 (16)	C(3)–C(4)	1.400 (18)				
Cl(1)–Ru–Cl(2)	164.53 (19)	C(11)–N–C(14)	110.2 (13)	C(1)–Fe–C(8)	163.5 (6)	Fe–C(3)–C(2)	71.9 (7)
Cl(1)–Ru–P(1)	92.59 (19)	C(13)–N–C(14)	108.9 (14)	C(1)–Fe–C(9)	128.0 (6)	C(4)–C(3)–C(2)	108.9 (9)
Cl(1)–Ru–P(2)	90.12 (16)	N–C(11)–C(12)	114.7 (15)	C(1)–Fe–C(10)	109.7 (5)	Fe–C(4)–C(3)	71.8 (7)
Cl(1)–Ru–N	89.1 (3)	N–C(11)–C(2)	108.5 (12)	C(1)–Fe–C(6)	121.7 (6)	Fe–C(4)–C(5)	72.2 (7)
Cl(2)–Ru–P(1)	102.67 (20)	C(12)–C(11)–C(2)	111.1 (13)	C(2)–Fe–C(7)	118.5 (6)	C(3)–C(4)–C(5)	113.2 (10)
Cl(2)–Ru–P(2)	88.03 (18)	P(1)–C(15)–C(16)	115.6 (11)	C(2)–Fe–C(8)	155.3 (6)	Fe–C(5)–C(4)	68.5 (7)
Cl(2)–Ru–N	86.6 (3)	P(1)–C(15)–C(17)	112.6 (11)	C(2)–Fe–C(9)	162.9 (7)	Fe–C(5)–C(1)	68.4 (7)
P(1)–Ru–P(2)	106.30 (18)	C(16)–C(15)–C(17)	110.0 (15)	C(2)–Fe–C(10)	121.3 (6)	C(4)–C(5)–C(1)	102.9 (10)
P(1)–Ru–N	97.0 (4)	P(1)–C(18)–C(19)	115.9 (11)	C(2)–Fe–C(6)	103.8 (5)	Fe–C(1)–P(1)	139.7 (7)
P(2)–Ru–N	156.7 (4)	P(1)–C(18)–C(20)	114.5 (13)	C(7)–Fe–C(8)	41.0 (7)	Fe–C(1)–C(5)	67.2 (7)
C(3)–Fe–C(4)	40.2 (5)	C(19)–C(18)–C(20)	106.9 (14)	C(7)–Fe–C(9)	69.8 (7)	Fe–C(1)–C(2)	71.4 (7)
C(3)–Fe–C(5)	68.3 (5)	P(2)–C(26)–C(21)	116.4 (9)	C(7)–Fe–C(10)	68.9 (6)	P(1)–C(1)–C(5)	120.7 (9)
C(3)–Fe–C(1)	67.0 (4)	P(2)–C(26)–C(25)	123.3 (9)	C(7)–Fe–C(6)	40.9 (6)	P(1)–C(1)–C(2)	129.4 (11)
C(3)–Fe–C(2)	39.7 (5)	C(21)–C(26)–C(25)	120.0 (10)	C(8)–Fe–C(9)	39.8 (7)	C(5)–C(1)–C(2)	107.5 (9)
C(3)–Fe–C(7)	103.0 (5)	C(26)–C(21)–C(22)	120.0 (11)	C(8)–Fe–C(10)	69.8 (7)	Fe–C(2)–C(11)	121.5 (9)
C(3)–Fe–C(8)	120.9 (6)	C(21)–C(22)–C(23)	120.0 (10)	C(8)–Fe–C(6)	69.4 (6)	Fe–C(2)–C(3)	68.4 (7)
C(3)–Fe–C(9)	156.9 (7)	C(22)–C(23)–C(24)	120.0 (11)	C(9)–Fe–C(10)	45.1 (7)	Fe–C(2)–C(1)	69.1 (8)
C(3)–Fe–C(10)	154.3 (6)	C(23)–C(24)–C(25)	120.0 (11)	C(9)–Fe–C(6)	72.1 (6)	C(11)–C(2)–C(3)	126.1 (11)
C(3)–Fe–C(6)	117.5 (6)	C(26)–C(25)–C(24)	120.0 (10)	C(10)–Fe–C(6)	40.7 (7)	C(11)–C(2)–C(1)	126.0 (12)
C(4)–Fe–C(5)	39.3 (5)	P(2)–C(27)–C(28)	121.0 (9)	Ru–P(1)–C(15)	118.3 (7)	C(3)–C(2)–C(1)	107.4 (10)
C(4)–Fe–C(1)	68.3 (4)	P(2)–C(27)–C(32)	118.9 (9)	Ru–P(1)–C(18)	117.6 (5)	Fe–C(7)–C(8)	68.6 (9)
C(4)–Fe–C(2)	67.6 (5)	C(28)–C(27)–C(32)	120.0 (9)	Ru–P(1)–C(1)	107.1 (5)	Fe–C(7)–C(6)	70.8 (8)
C(4)–Fe–C(7)	119.6 (5)	C(27)–C(28)–C(29)	120.0 (10)	C(15)–P(1)–C(18)	106.0 (8)	C(8)–C(7)–C(6)	108.9 (12)
C(4)–Fe–C(8)	107.6 (6)	C(28)–C(29)–C(30)	120.0 (11)	C(15)–P(1)–C(1)	99.5 (7)	Fe–C(8)–C(7)	70.4 (9)
C(4)–Fe–C(9)	123.2 (6)	C(29)–C(30)–C(31)	120.0 (9)	C(18)–P(1)–C(1)	106.2 (7)	Fe–C(8)–C(9)	72.1 (10)
C(4)–Fe–C(10)	164.7 (6)	C(30)–C(31)–C(32)	120.0 (10)	Ru–P(2)–C(26)	99.3 (4)	C(7)–C(8)–C(9)	113.2 (14)
C(4)–Fe–C(6)	153.7 (6)	C(27)–C(32)–C(31)	120.0 (10)	Ru–P(2)–C(27)	124.5 (4)	Fe–C(9)–C(8)	68.1 (10)
C(5)–Fe–C(1)	44.3 (5)	P(2)–C(33)–C(34)	118.2 (10)	Ru–P(2)–C(33)	123.0 (4)	Fe–C(9)–C(10)	67.1 (8)
C(5)–Fe–C(2)	70.4 (5)	P(2)–C(33)–C(38)	121.8 (8)	C(26)–P(2)–C(27)	103.7 (6)	C(8)–C(9)–C(10)	102.9 (13)
C(5)–Fe–C(7)	155.4 (6)	C(34)–C(33)–C(38)	120.0 (10)	C(26)–P(2)–C(33)	98.8 (6)	Fe–C(10)–C(9)	67.7 (8)
C(5)–Fe–C(8)	122.3 (6)	C(33)–C(34)–C(35)	120.0 (12)	C(27)–P(2)–C(33)	102.3 (5)	Fe–C(10)–C(6)	70.2 (8)
C(5)–Fe–C(9)	108.8 (6)	C(34)–C(35)–C(36)	120.0 (11)	Ru–N–C(11)	111.0 (10)	C(9)–C(10)–C(6)	107.5 (12)
C(5)–Fe–C(10)	128.5 (6)	C(35)–C(36)–C(37)	120.0 (12)	Ru–N–C(13)	118.1 (9)	Fe–C(6)–C(7)	68.2 (9)
C(5)–Fe–C(6)	163.6 (6)	C(36)–C(37)–C(38)	120.0 (13)	Ru–N–C(14)	98.1 (9)	Fe–C(6)–C(10)	69.1 (9)
C(1)–Fe–C(2)	39.5 (5)	C(33)–C(38)–C(37)	120.0 (11)	C(11)–N–C(13)	109.8 (12)	C(7)–C(6)–C(10)	107.4 (13)
C(1)–Fe–C(7)	155.2 (7)	Fe–C(3)–C(4)	68.1 (7)				

[a] And all Ph C–C.

X-ray Data Collection and Reduction for 5. Precession photography (Cu Kα radiation) indicated a orthorhombic unit cell, and the space group was confirmed as $P2_12_12_1$ (No 19).[16] A deep-red block was chosen for data collection on a Nicolet R3M diffractometer at 173 ± 5 K, using graphite-monochromated Mo Kα radiation. The data were corrected for Lorentz and polarization factors using SHELXTL.[17] Empirical absorption corrections were applied similarly with transmission factors of 0.890 (max) 0.472 (min). Other details of the crystals, data collection and structure solution are summarized in Table I. The structure was solved by Patterson methods using the PATT option of SHELXS-86.[18] The resulting Fourier map revealed the location of the Ru, Fe, P, and Cl atoms. The remaining non-hydrogen atoms were found in subsequent different Fourier least-squares refinement cycles.[19] Hydrogen atoms on the organic moieties were included in calculated positions (d(C–H) 0.98 Å) with fixed isotropic thermal parameters. Weighted refinement continued with all non-hydrogen atoms assigned anisotropic thermal parameters. The function minimized was $\sum w(F_o - F_c)^2$ using a version of SHELX-76 amended for large structures.[20] Refinement converged with $R = 0.0770$ and $R_w = 0.0786$. A difference Fourier synthesis following the final refinement showed a number of high peaks in the vicinity of the Ru, P, and Cl atoms. Of these, only one was in a suitable location to be considered as the H atom position.

Final positional and equivalent thermal parameters and selected bond lengths and angles, are listed in Tables VI and VII, respectively. Tables of thermal parameters, H-atom parameters, all bond lengths and angles, and observed and calculated structure factors are included in the deposited material (Tables SV–SVII); complete crystal data are given in Table SI.

Results and Discussion

Rodgers et al.[4] reported a study of the homogeneous hydrogenation of 1-hexene that is catalyzed by $RuCl_2(PPh_3)$(PPFA) (**2a**):

$$H_2 + \text{1-hexene} \xrightarrow[n\text{-butanol, 40 °C}]{RuCl_2(PPh_3)(PPFA)} \text{hexane} \qquad (1)$$

In an attempt to identify possible intermediates involved, reactions of **2a**, the catalyst precursor, with H_2 were carried out

(17) Sheldrick, G. M. SHELXTL, an integrated system for solving, refining, and displaying crystal structures from diffraction data. University of Göttingen, 1981.
(18) Sheldrick, G. M. SHELXS-86, program for the solution of crystal structures from diffraction data. University of Göttingen, 1986.
(19) Sheldrick, G. M. SHELX-76, program for crystal structure determination. University of Cambridge, 1976.
(20) Rabinovich, D.; Reich, K. SHELX400, a modification of SHELX-76 to allow the refinement of up to 400 atoms. Weizmann Institute of Science, Rehovot, Israel, 1979.

Table IV. Atomic Parameters x, y, z, and B_{iso} for the Non-Hydrogen Atoms of $(\eta^2\text{-}H_2)(isoPFA)Ru(\mu\text{-}Cl)_2(\mu\text{-}H)Ru(H)(PPh_3)_2 \cdot 3$ (1.5 C_6H_6)[a]

atom	x	y	z	B_{iso},[b] Å^2	atom	x	y	z	B_{iso},[b] Å^2
Ru(1)	0.74498 (4)	0.10046 (3)	0.697672 (17)	2.430 (18)	C(212)	0.8966 (5)	0.1271 (3)	0.94649 (23)	3.8 (3)
Ru(2)	0.74063 (4)	−0.06824 (3)	0.731212 (17)	2.246 (17)	C(213)	0.9550 (6)	0.2236 (4)	0.98252 (24)	5.0 (3)
Fe	0.44040 (8)	0.29738 (5)	0.64570 (4)	4.08 (4)	C(214)	1.0399 (6)	0.2862 (3)	0.9547 (3)	5.4 (3)
Cl(1)	0.93603 (11)	0.02732 (9)	0.67735 (6)	3.36 (6)	C(215)	1.0656 (5)	0.2504 (3)	0.8896 (3)	4.5 (3)
Cl(2)	0.61691 (12)	−0.06494 (8)	0.63165 (5)	3.32 (6)	C(216)	1.0080 (5)	0.1542 (3)	0.85385 (22)	3.5 (3)
P(1)	0.57945 (12)	0.16152 (9)	0.73593 (6)	2.71 (6)	C(221)	0.7616 (4)	−0.0922 (3)	0.89041 (19)	2.55 (23)
P(2)	0.85475 (12)	−0.03947 (8)	0.82974 (5)	2.42 (6)	C(222)	0.8067 (5)	−0.1419 (3)	0.92690 (21)	3.22 (25)
P(3)	0.70116 (12)	−0.23069 (8)	0.69740 (6)	2.52 (6)	C(223)	0.7298 (5)	−0.1791 (4)	0.97190 (24)	4.2 (3)
N	0.7640 (4)	0.1535 (3)	0.60499 (17)	3.19 (19)	C(224)	0.6078 (5)	−0.1646 (4)	0.98070 (24)	4.5 (3)
C(1)	0.5704 (4)	0.2557 (3)	0.69953 (21)	2.86 (22)	C(225)	0.5587 (5)	−0.1153 (4)	0.94517 (24)	4.3 (3)
C(2)	0.6136 (4)	0.2568 (3)	0.63523 (22)	3.13 (23)	C(226)	0.6353 (5)	−0.0800 (3)	0.89978 (23)	3.6 (3)
C(3)	0.6355 (5)	0.3528 (3)	0.63122 (24)	4.1 (3)	C(231)	1.0155 (4)	−0.0670 (3)	0.83039 (20)	2.53 (22)
C(4)	0.6062 (6)	0.4108 (3)	0.6911 (3)	4.9 (3)	C(232)	1.0574 (4)	−0.1099 (3)	0.77046 (22)	3.11 (24)
C(5)	0.5647 (5)	0.3517 (3)	0.73326 (23)	3.6 (3)	C(233)	1.1804 (5)	−0.1274 (3)	0.76835 (24)	3.9 (3)
C(6)	0.2408 (6)	0.2132 (5)	0.6310 (4)	7.0 (4)	C(234)	1.2649 (5)	−0.1027 (4)	0.8259 (3)	4.1 (3)
C(7)	0.2920 (6)	0.2112 (5)	0.5692 (3)	7.4 (4)	C(235)	1.2264 (5)	−0.0581 (4)	0.88529 (24)	4.3 (3)
C(8)	0.3358 (7)	0.3101 (5)	0.5674 (3)	7.1 (4)	C(236)	1.1032 (5)	−0.0403 (3)	0.88801 (22)	3.5 (3)
C(9)	0.3129 (7)	0.3689 (5)	0.6279 (3)	7.2 (4)	C(311)	0.6944 (4)	−0.2992 (3)	0.75779 (20)	2.81 (22)
C(10)	0.2555 (6)	0.3095 (5)	0.6665 (4)	7.4 (4)	C(312)	0.8071 (5)	−0.3159 (3)	0.78216 (22)	3.6 (3)
C(11)	0.6083 (5)	0.2309 (4)	0.82694 (22)	3.8 (3)	C(313)	0.8019 (6)	−0.3664 (4)	0.82755 (24)	4.4 (3)
C(12)	0.7394 (6)	0.3141 (4)	0.8470 (3)	5.4 (3)	C(314)	0.6814 (6)	−0.4009 (4)	0.85112 (24)	4.9 (3)
C(13)	0.5982 (6)	0.1627 (4)	0.86932 (25)	5.8 (4)	C(315)	0.5690 (6)	−0.3847 (4)	0.8286 (3)	4.7 (3)
C(14)	0.4073 (5)	0.0783 (3)	0.72882 (25)	3.7 (3)	C(316)	0.5745 (5)	−0.3344 (3)	0.78205 (23)	3.8 (3)
C(15)	0.3093 (5)	0.1254 (4)	0.7668 (3)	5.1 (3)	C(321)	0.8096 (4)	−0.2795 (3)	0.63727 (20)	2.71 (22)
C(16)	0.3497 (5)	0.0243 (4)	0.6558 (3)	4.6 (3)	C(322)	0.8374 (5)	−0.3674 (3)	0.62864 (23)	3.58 (25)
C(17)	0.6371 (5)	0.1724 (3)	0.58314 (22)	3.46 (25)	C(323)	0.9137 (5)	−0.3993 (4)	0.57933 (25)	4.2 (3)
C(18)	0.6369 (6)	0.1887 (4)	0.51430 (24)	5.3 (3)	C(324)	0.9624 (5)	−0.3453 (4)	0.53833 (24)	4.5 (3)
C(19)	0.8821 (5)	0.2411 (4)	0.6184 (3)	4.7 (3)	C(325)	0.9366 (5)	−0.2596 (4)	0.54522 (24)	4.6 (3)
C(20)	0.7896 (6)	0.0746 (4)	0.5495 (3)	5.3 (3)	C(326)	0.8599 (5)	−0.2263 (3)	0.59504 (22)	3.6 (3)
C(21)[a]	0.0525 (9)	0.4653 (6)	0.7894 (4)	11.6 (6)	C(331)	0.5340 (4)	−0.2968 (3)	0.64732 (21)	2.82 (23)
C(22)[a]	0.0780 (9)	0.4982 (5)	0.8553 (4)	10.0 (6)	C(332)	0.5128 (5)	−0.3828 (3)	0.59566 (23)	3.9 (3)
C(23)[a]	0.1550 (9)	0.5900 (6)	0.8859 (4)	10.7 (6)	C(333)	0.3880 (5)	−0.4316 (4)	0.55938 (24)	4.6 (3)
C(24)[a]	0.2054 (9)	0.6493 (5)	0.8478 (5)	12.2 (7)	C(334)	0.2823 (5)	−0.3955 (4)	0.57302 (25)	4.4 (3)
C(25)[a]	0.1777 (10)	0.6126 (7)	0.7801 (6)	14.3 (8)	C(335)	0.3022 (5)	−0.3106 (4)	0.6236 (3)	4.6 (3)
C(26)[a]	0.0993 (11)	0.5207 (7)	0.7502 (5)	13.6 (8)	C(336)	0.4260 (5)	−0.2613 (3)	0.66010 (23)	3.8 (3)
C(27)[a]	0.5538 (7)	0.5930 (4)	0.0400 (3)	7.3 (4)	H(1)	0.841 (4)	0.171 (3)	0.7566 (21)	5.4 (12)
C(28)[a]	0.5466 (7)	0.4290 (5)	0.0088 (4)	8.0 (5)	H(2)	0.824 (4)	0.201 (3)	0.7336 (21)	5.1 (12)
C(29)[a]	0.6017 (7)	0.5245 (5)	0.0496 (4)	8.2 (4)	H(12)	0.735 (4)	0.034 (3)	0.7521 (20)	4.7 (11)
C(211)	0.9220 (4)	0.0901 (3)	0.88134 (20)	2.70 (22)	H(13)	0.615 (4)	−0.097 (3)	0.7638 (18)	3.6 (10)

[a] Atoms C21–C29 are those of 1.5 C_6H_6 solvate molecules. [b] As in footnote *a* of Table II.

in the absence of substrate, and it was found that *n*-butanol solutions of **2a** absorb slightly more than 0.5 mol of H_2/mol of Ru at 40 °C at several pressures, the solution color changing from green to red.[4] These reactions at constant hydrogen pressure follow pseudo-first-order behavior. Hydrides were not detected in the butanol solutions, or benzene solutions where reaction with H_2 was slow and incomplete. Attempts to isolate solids from the butanol solutions by solvent evaporation, even under H_2, resulted in slow regeneration of the green color of **2a**.

Subsequent studies revealed that **2a** reacts with H_2 in DMA and toluene/methanol, and at the time the present work was initiated it appeared that a hydride was formed at least in toluene/methanol (evidenced by a broad, high-field ^{1}H NMR signal); there was an indication of reversibility in the reactions in DMA and in butanol.[21] It is clear that the presence of a polar solvent such as DMA or alcohol has a pronounced effect on the reactivity of **2a** toward H_2, and such solvents are known to promote monohydride formation via a net heterolytic cleavage of H_2.[22]

We now find that the reaction of **2a** with dihydrogen (~3 atm) in toluene is complete at 20 °C: the products remain unidentified, but it seems that no hydrides are present, as judged by the absence of high-field ^{1}H NMR signals. In butanol, the solvent used in the catalyzed hydrogenation studies, reaction with hydrogen results in ligand redistribution to afford some $(\eta^2\text{-}H_2)(PPh_3)_2Ru(\mu\text{-}Cl)_2(\mu\text{-}H)RuH(PPh_3)_2$ (**4**), a compound that is discussed in more detail below. However, the principal product is a yellow solid, **8**, that when dissolved in toluene or CH_2Cl_2 liberates BuOH and H_2 (1 mol per Ru for the suggested formulation), with regeneration of green **2a**. This phenomenon can be monitored by using NMR spectroscopy. The yellow hydride (^{1}H NMR: δ −20.4 (t)) is stable in butanol under 1 atm of H_2. These and other observations indicate that an equilibrium exists between **2a** and **8** as suggested by eq 2. A plausible, tentative

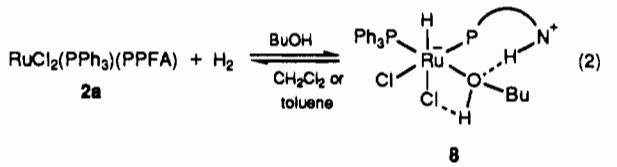

(2)

structure for **8** involves a zwitterionic species stabilized by coordinated butanol. In CH_2Cl_2 or toluene, loss of the coordinated butanol could result in destabilization and reversal of the reaction between the hydride and nitrogen-stabilized proton to give H_2 and complex **2a**, as observed in gas evolution experiments. The presence of a hydride ligand, cis to two almost equivalent mutually cis phosphine ligands, is consistent with the observed highfield pseudo-triplet ($^2J_{PH}$ = 32 Hz) in the ^{1}H NMR spectrum and the magnitude ($^2J_{PP}$ = 40 Hz) of the ^{31}P{^{1}H} NMR coupling constants.[23] The pale yellow color of this hydride is consistent with a six-coordinate complex; five-coordinate Ru(II) hydrides

(21) Thorburn, I. S.; Butler, I. R. Unpublished results.
(22) James, B. R. In *Comprehensive Organometallic Chemistry*; Wilkinson, G., Stone, F. G. A., Abel, E. W., Eds.; Pergamon, Oxford, England, 1982; Vol. 8, Chapter 51.
(23) (a) Kaesz, H. D.; Saillant, R. B. *Chem. Rev.* **1972**, *72*, 231. (b) Chaudret, B. N.; Cole-Hamilton, D. J.; Nohr, R. S.; Wilkinson, G. *J. Chem. Soc., Dalton Trans.* **1977**, 1546. (c) Cole-Hamilton, D. J.; Wilkinson, G. *Nouv. J. Chim.* **1977**, *1*, 142.

Table V. Bond Lengths (Å) and Angles (deg) Involving the Ru-Bonded Atoms of $(\eta^2\text{-}H_2)$(isoPFA)Ru$(\mu\text{-}Cl)_2(\mu\text{-}H)$Ru(H)$(PPh_3)_2$ (3)

Ru(1)–Ru(2)	2.8108 (16)	Ru(2)–Cl(1)	2.6198 (23)
Ru(1)–Cl(1)	2.5279 (22)	Ru(2)–Cl(2)	2.4534 (18)
Ru(1)–Cl(2)	2.4351 (24)	Ru(2)–P(2)	2.2294 (19)
Ru(1)–P(1)	2.2403 (21)	Ru(2)–P(3)	2.2492 (20)
Ru(1)–N	2.300 (4)	Ru(2)–H(12)	1.49 (4)
Ru(1)–H(1)	1.50 (4)	Ru(2)–H(13)	1.50 (4)
Ru(1)–H(2)	1.47 (4)	H(1)–H(2)	0.80 (6)
Ru(1)–H(12)	1.71 (4)		

Ru(2)–Ru(1)–Cl(1)	58.49 (5)	H(2)–Ru(1)–H(12)	107.6 (21)
Ru(2)–Ru(1)–Cl(2)	55.21 (5)	Ru(1)–Ru(2)–Cl(1)	55.35 (5)
Ru(2)–Ru(1)–P(1)	113.40 (6)	Ru(1)–Ru(2)–Cl(2)	54.60 (5)
Ru(2)–Ru(1)–N	138.46 (9)	Ru(1)–Ru(2)–P(2)	114.33 (6)
Ru(2)–Ru(1)–H(1)	96.2 (17)	Ru(1)–Ru(2)–P(3)	148.16 (4)
Ru(2)–Ru(1)–H(2)	127.4 (17)	Ru(1)–Ru(2)–H(12)	30.7 (16)
Ru(2)–Ru(1)–H(12)	26.5 (13)	Ru(1)–Ru(2)–H(13)	107.6 (14)
Cl(1)–Ru(1)–Cl(2)	80.92 (8)	Cl(1)–Ru(2)–Cl(2)	78.76 (7)
Cl(1)–Ru(1)–P(1)	168.54 (4)	Cl(1)–Ru(2)–P(2)	98.02 (8)
Cl(1)–Ru(1)–N	94.66 (11)	Cl(1)–Ru(2)–P(3)	114.36 (7)
Cl(1)–Ru(1)–H(1)	82.6 (17)	Cl(1)–Ru(2)–H(12)	74.9 (16)
Cl(1)–Ru(1)–H(2)	98.6 (17)	Cl(1)–Ru(2)–H(13)	162.8 (14)
Cl(1)–Ru(1)–H(12)	74.8 (14)	Cl(2)–Ru(2)–P(2)	168.32 (4)
Cl(2)–Ru(1)–P(1)	101.22 (8)	Cl(2)–Ru(2)–P(3)	95.19 (7)
Cl(2)–Ru(1)–N	92.35 (11)	Cl(2)–Ru(2)–H(12)	78.5 (15)
Cl(2)–Ru(1)–H(1)	151.3 (17)	Cl(2)–Ru(2)–H(13)	93.3 (14)
Cl(2)–Ru(1)–H(2)	176.6 (17)	P(2)–Ru(2)–P(3)	96.35 (7)
Cl(2)–Ru(1)–H(12)	75.6 (13)	P(2)–Ru(2)–H(12)	89.9 (15)
P(1)–Ru(1)–N	96.49 (11)	P(2)–Ru(2)–H(13)	86.7 (14)
P(1)–Ru(1)–H(1)	90.8 (17)	P(3)–Ru(2)–H(12)	167.8 (15)
P(1)–Ru(1)–H(2)	79.9 (17)	P(3)–Ru(2)–H(13)	81.3 (14)
P(1)–Ru(1)–H(12)	94.7 (14)	H(12)–Ru(2)–H(13)	88.6 (21)
N–Ru(1)–H(1)	112.3 (17)	Ru(1)–Cl(1)–Ru(2)	66.16 (6)
N–Ru(1)–H(2)	84.3 (17)	Ru(1)–Cl(2)–Ru(2)	70.20 (6)
N–Ru(1)–H(12)	165.0 (13)	Ru(1)–H(1)–H(2)	72 (4)
H(1)–Ru(1)–H(2)	31.3 (24)	Ru(1)–H(2)–H(1)	76 (4)
H(1)–Ru(1)–H(12)	77.5 (21)	Ru(1)–H(12)–Ru(2)	122 (3)

are typically intensely red.[23b] The microanalytical results for the solid are reasonably close to those expected for the suggested composition, **8**. A conductivity measurement indicates the presence of ionic material, presumably impurities. The presence of two overlapping doublets in the $^{31}P\{^1H\}$ NMR spectrum is probably due to the presence of diastereomers in solution; the PPFA ligand may be *R,S* or *S,R*, and the Ru center of **8** is also chiral. Additional ^1H resonances for possible diastereomers are not seen and are considered not to be resolved; a similar finding pertains for diastereomers of **3** (see below).

The reaction of eq 2 implies heterolytic cleavage of H_2 promoted by the amine functionality of the coordinated PPFA ligand; indeed, one goal of our original P–N ligand work was to determine if such a reaction might occur. Direct data to support heterolytic cleavage of H_2 at a metal center are becoming more available,[24] and the possibility is particularly important for Ru(II) centers where monohydride formation within a mononuclear species would otherwise have to involve Ru(IV) dihydride intermediates.[4] Protonation of the amine group in the reaction of the analogous complex, $RuCl_2(PPh_3)$(isoPFA) (**2b**), in its reaction with H_2 in benzene/methanol could be the first step in the ultimate formation of $H_2NMe_2^+Cl^-$. This reaction, which is described below, could proceed through an intermediate such as **8**.

In the belief that these studies might be facilitated by using a P–N ligand containing a more basic phosphine moiety, the complex $RuCl_2(PPh_3)$(isoPFA) (**2b**) was synthesized by displacing PPh_3 from $RuCl_2(PPh_3)_3$ with isoPFA. Complex **2b**, like **2a**, is green, and the analytical and spectroscopic data are in accord with the formulation. The crystal structure of **2b** is discussed below.

(24) (a) Fryzuk, M. D.; MacNeil, P. A. *Organometallics* **1983**, *2*, 682. (b) Albeniz, A. C.; Heinekey, D. M.; Crabtree, R. H. *Inorg. Chem.* **1991**, *30*, 3632. (c) Chinn, M. S.; Heinekey, D. M. *J. Am. Chem. Soc.* **1990**, *112*, 5166.

Table VI. Final Positional and Equivalent Thermal Parameters for the Non-Hydrogen Atoms of RuH(Cl)(PPh_3)(isoPFA) (**5**)

atom	*x/a*	*y/b*	*z/c*	U_{eq}, Å^2
Ru(1)	0.8973 (1)	0.9571 (1)	0.1404 (0)	0.021
Fe(1)	0.7410 (2)	0.6583 (1)	0.1428 (1)	0.030
P(1)	0.7172 (3)	0.8848 (2)	0.1238 (1)	0.021
P(2)	0.8517 (3)	1.0693 (2)	0.0856 (1)	0.022
Cl(1)	0.9399 (5)	1.0363 (2)	0.2329 (2)	0.036
N(1)	1.027 (1)	0.8588 (7)	0.1836 (5)	0.031
C(1)	0.740 (1)	0.7827 (8)	0.1581 (6)	0.026
C(2)	0.862 (2)	0.7481 (8)	0.1769 (6)	0.029
C(3)	0.843 (2)	0.6888 (8)	0.2218 (6)	0.035
C(4)	0.699 (2)	0.6838 (9)	0.2325 (6)	0.035
C(5)	0.637 (2)	0.7414 (8)	0.1925 (6)	0.033
C(6)	0.840 (2)	0.5904 (8)	0.0774 (8)	0.048
C(7)	0.719 (2)	0.6234 (9)	0.0518 (7)	0.053
C(8)	0.609 (2)	0.594 (1)	0.0883 (9)	0.059
C(9)	0.662 (2)	0.5445 (9)	0.1347 (8)	0.049
C(10)	0.804 (2)	0.5428 (9)	0.1276 (8)	0.054
C(11)	1.000 (1)	0.7769 (8)	0.1532 (6)	0.029
C(12)	1.109 (2)	0.7133 (8)	0.1643 (6)	0.035
C(13)	1.161 (1)	0.8885 (9)	0.1643 (8)	0.038
C(14)	1.021 (2)	0.8514 (9)	0.2513 (6)	0.038
C(15)	0.651 (2)	0.8650 (7)	0.0450 (6)	0.034
C(16)	0.528 (2)	0.8098 (9)	0.0447 (8)	0.049
C(17)	0.760 (2)	0.8326 (9)	0.0043 (6)	0.038
C(18)	0.562 (1)	0.9186 (9)	0.1662 (7)	0.038
C(19)	0.493 (1)	0.9909 (8)	0.1365 (9)	0.042
C(20)	0.595 (2)	0.9339 (9)	0.2323 (6)	0.040
C(21)	0.783 (2)	1.0640 (7)	0.0067 (6)	0.028
C(22)	0.862 (2)	1.0426 (9)	−0.0430 (6)	0.039
C(23)	0.804 (2)	1.033 (1)	−0.1002 (7)	0.052
C(24)	0.668 (2)	1.047 (1)	−0.1101 (7)	0.047
C(25)	0.589 (2)	1.0702 (9)	−0.0607 (6)	0.042
C(26)	0.646 (2)	1.0779 (9)	−0.0027 (6)	0.035
C(27)	0.763 (1)	1.1594 (8)	0.1135 (6)	0.030
C(28)	0.711 (2)	1.1619 (8)	0.1718 (7)	0.034
C(29)	0.639 (2)	1.232 (1)	0.1928 (9)	0.056
C(30)	0.621 (2)	1.2966 (9)	0.1525 (7)	0.051
C(31)	0.674 (2)	1.294 (1)	0.0950 (9)	0.059
C(32)	0.741 (2)	1.2266 (8)	0.0747 (8)	0.043
C(33)	1.026 (1)	1.1089 (8)	0.0777 (5)	0.022
C(34)	1.123 (1)	1.0608 (8)	0.0511 (6)	0.031
C(35)	1.257 (2)	1.0881 (9)	0.0477 (8)	0.046
C(36)	1.294 (2)	1.164 (1)	0.0702 (8)	0.053
C(37)	1.195 (2)	1.210 (1)	0.0983 (8)	0.048
C(38)	1.064 (2)	1.1851 (9)	0.1015 (7)	0.037

The main product from the reaction of **2b** in benzene/methanol (10:1) is the novel binuclear dihydride complex **3**. The structure of $(\eta^2\text{-}H_2)$(isoPFA)Ru$(\mu\text{-}Cl)_2(\mu\text{-}H)RuH(PPh_3)_2$ (**3**), Figure 3, shows that considerable redistribution of ligands again occurs. The isolation of $H_2NMe_2^+Cl^-$ from the reaction solution is mentioned above. The residual ferrocene moiety was not isolated and at least one other ruthenium hydride species (the black-red crystals, $\delta_H = -21.8$ q in $CDCl_3$ at 20 °C), so far unidentified, is produced in this reaction. Complex **3** is also produced in DMA/C_6D_6 along with $(\eta^2\text{-}H_2)(PPh_3)_2Ru(\mu\text{-}Cl)_2(\mu\text{-}H)RuH(PPh_3)_2$ (**4**) and RuH(Cl)(PPh_3)(isoPFA) (**5**). The structure of **5** is discussed below. In DMA alone, the main product is **4**, while if PPh_3 is added to the reaction mixture the product is Ru(H)Cl$(PPh_3)_3$.

It is important to note that, in the absence of added base, complexes **2a** and **2b** react with hydrogen in butanol, methanol/benzene, or DMA to give, among other products, the dinuclear $\eta^2\text{-}H_2$ complexes **4** and **3**, respectively. In contrast, the complexes $Ru_2Cl_4(PR_3)_4$ (R = Ph, *p*-tolyl) react with hydrogen to give dinuclear $\eta^2\text{-}H_2$ complexes $(\eta^2\text{-}H_2)(PR_3)_2Ru(\mu\text{-}Cl)_2(\mu\text{-}H)RuH(PR_3)_2$ (R = Ph, **4**; R = *p*-tolyl, **7**) only in the presence of Proton Sponge, a stronger base than DMA.[8] This difference in reactivity toward H_2 must be in part related to involvement of the ligand–amine functionality that accepts a proton. This probably occurs in DMA as well, although isoPFA fragments were not isolated from reactions in this system.

Complex **3** is well characterized by means of NMR spectroscopy, a solid-state structure, and microanalysis.[5] The complex

Table VII. Selected Bond Lengths (Å) and Angles (deg) for $RuH(Cl)(PPh_3)$(isoPFA) (**5**)

Ru(1)–P(1)	2.178 (3)	P(2)–C(33)	1.85 (1)
Ru(1)–P(2)	2.249 (3)	N(1)–C(11)	1.53 (2)
Ru(1)–Cl(1)	2.440 (3)	N(1)–C(13)	1.48 (2)
Ru(1)–N(1)	2.27 (1)	N(1)–C(14)	1.48 (2)
Fe(1)–C(1)	2.08 (1)	C(1)–C(2)	1.40 (2)
Fe(1)–C(2)	2.05 (1)	C(1)–C(5)	1.44 (2)
Fe(1)–C(3)	2.06 (2)	C(2)–C(3)	1.40 (2)
Fe(1)–C(4)	2.04 (1)	C(2)–C(11)	1.53 (2)
Fe(1)–C(5)	2.03 (1)	C(3)–C(4)	1.45 (2)
Fe(1)–C(6)	2.06 (2)	C(4)–C(5)	1.42 (2)
Fe(1)–C(7)	2.08 (2)	C(11)–C(12)	1.53 (2)
Fe(1)–C(8)	2.06 (2)	C(15)–C(16)	1.52 (2)
Fe(1)–C(9)	2.05 (1)	C(15)–C(17)	1.49 (2)
Fe(1)–C(10)	2.04 (2)	C(18)–C(19)	1.52 (2)
P(1)–C(1)	1.86 (1)	C(18)–C(20)	1.50 (2)
P(1)–C(15)	1.87 (1)		
P(1)–C(18)	1.88 (1)		
P(2)–C(21)	1.85 (1)		
P(2)–C(27)	1.83 (1)		

P(1)–Ru(1)–P(2)	101.5 (1)	C(11)–N(1)–C(13)	109 (1)
P(1)–Ru(1)–Cl(1)	124.9 (1)	C(11)–N(1)–C(14)	110 (1)
P(1)–Ru(1)–N(1)	98.0 (3)	C(13)–N(1)–C(14)	109 (1)
P(2)–Ru(1)–Cl(1)	91.9 (1)	Fe(1)–C(1)–P(1)	146.3 (7)
P(2)–Ru(1)–N(1)	157.1 (3)	Fe(1)–C(1)–C(2)	68.9 (8)
Cl(1)–Ru(1)–N(1)	86.7 (3)	Fe(1)–C(1)–C(5)	67.5 (7)
C(1)–Fe(1)–C(2)	39.5 (6)	P(1)–C(1)–C(2)	126 (1)
C(1)–Fe(1)–C(3)	68.0 (5)	P(1)–C(1)–C(5)	123 (1)
C(1)–Fe(1)–C(4)	69.0 (5)	C(2)–C(1)–C(5)	105 (1)
C(1)–Fe(1)–C(5)	41.0 (5)	Fe(1)–C(2)–C(1)	71.6 (8)
C(2)–Fe(1)–C(3)	39.8 (5)	Fe(1)–C(2)–C(3)	70.6 (8)
C(2)–Fe(1)–C(4)	67.9 (6)	Fe(1)–C(2)–C(11)	128.6 (9)
C(2)–Fe(1)–C(5)	67.3 (6)	C(1)–C(2)–C(3)	112 (1)
C(3)–Fe(1)–C(4)	41.4 (6)	C(1)–C(2)–C(11)	122 (1)
C(3)–Fe(1)–C(5)	68.7 (6)	C(3)–C(2)–C(11)	125 (1)
C(4)–Fe(1)–C(5)	41.0 (6)	Fe(1)–C(3)–C(2)	69.7 (8)
Ru(1)–P(1)–C(1)	109.3 (5)	Fe(1)–C(3)–C(4)	68.7 (9)
Ru(1)–P(1)–C(15)	122.3 (5)	C(2)–C(3)–C(4)	106 (1)
Ru(1)–P(1)–C(18)	115.3 (5)	Fe(1)–C(4)–C(3)	69.9 (8)
C(1)–P(1)–C(15)	104.7 (6)	Fe(1)–C(4)–C(5)	69.0 (8)
C(1)–P(1)–C(18)	99.9 (6)	C(3)–C(4)–C(5)	106 (1)
C(15)–P(1)–C(18)	102.6 (7)	Fe(1)–C(5)–C(1)	71.5 (8)
Ru(1)–P(2)–C(21)	121.8 (4)	Fe(1)–C(5)–C(4)	70.0 (8)
Ru(1)–P(2)–C(27)	126.1 (4)	C(1)–C(5)–C(4)	109 (1)
Ru(1)–P(2)–C(33)	98.8 (4)	N(1)–C(11)–C(2)	106 (1)
C(21)–P(2)–C(27)	99.7 (6)	N(1)–C(11)–C(12)	114 (1)
C(21)–P(2)–C(33)	105.9 (6)	C(2)–C(11)–C(12)	111 (1)
C(27)–P(2)–C(33)	101.1 (6)	P(1)–C(15)–C(16)	112 (1)
Ru(1)–N(1)–C(11)	110.7 (8)	P(1)–C(15)–C(17)	111 (1)
Ru(1)–N(1)–C(13)	98.9 (8)	C(16)–C(15)–C(17)	111 (1)
Ru(1)–N(1)–C(14)	116.8 (9)	P(1)–C(18)–C(19)	113 (1)
		P(1)–C(18)–C(20)	110 (1)
		C(19)–C(18)–C(20)	112 (1)

is stable in CD_2Cl_2 solution for hours at 20 °C in an NMR tube sealed under vacuum, but after a few days the sample decomposes to **4** and other phosphorus-containing products, as judged by NMR spectroscopy. However, when sealed under hydrogen in CD_2Cl_2, there is no change in the ^1H NMR spectrum of **3** after several weeks.

X-ray Structures of Complexes 2b, 3, and 5. Drawings of complexes **2b** and **3** showing the numbering schemes are presented in Figures 2 and 3, respectively. In **2b**, the Ru(II) is in a distorted square pyramidal environment; the PPh_3, the $-NMe_2$, and the two trans chloro groups describe the base of the pyramid, and the apical position is occupied by the $-P(i\text{-}Pr)_2$ group. The intramolecular distance between Ru and H(21) on the PPh_3 ligand is 2.84 Å, as depicted in Figure 4, and on the basis of the van der Waals radii of H (1.2 Å) and Ru (1.6 Å),[25] it seems that there is a van der Waals interaction involving these two atoms. Figure 4 reveals also that H(21) in trans to P(1), and, therefore, **2b** has

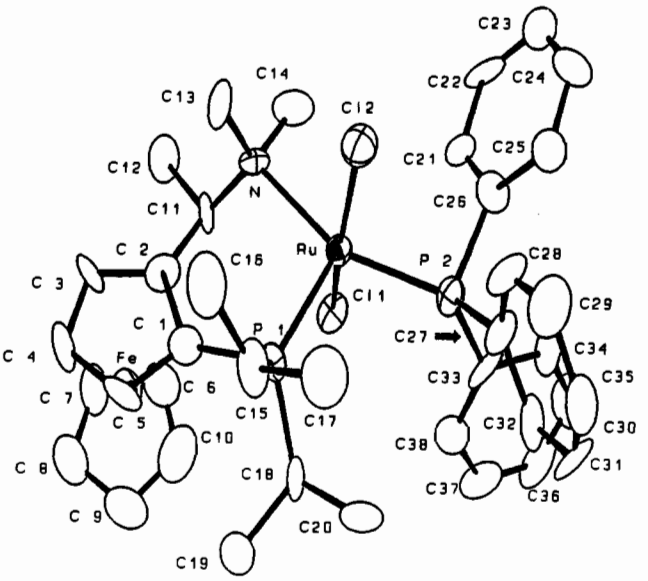

Figure 2. ORTEP plot of the structure of **2b**.

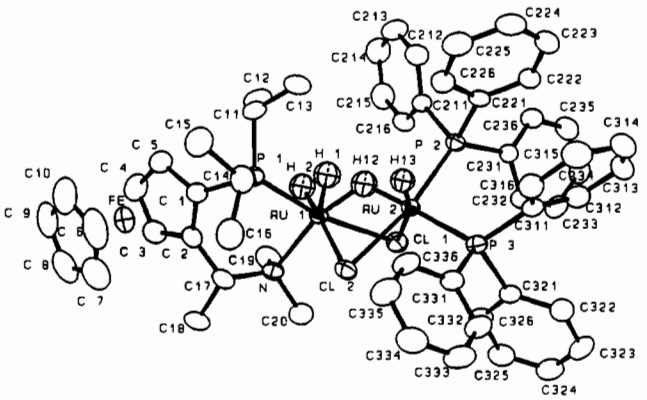

Figure 3. ORTEP plot of the structure of **3**.

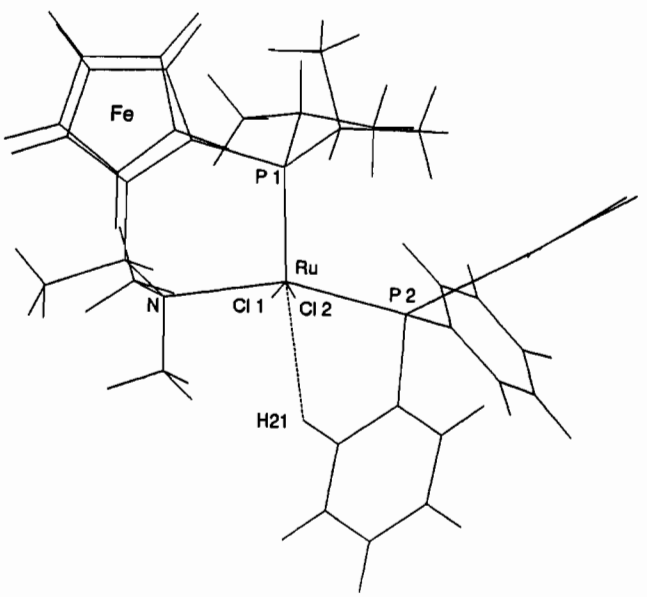

Figure 4. Diagram of the structure of **2b**, highlighting the van der Waals interaction between H(21) and Ru.

a square pyramid structure in which the sixth octahedral position is blocked by H(21). This structural feature was also reported for the crystal structure of the red-brown $RuCl_2(PPh_3)_3$.[26] Presumably the structure of **2a** is similar to that of **2b**; however,

(25) Huheey, J. E. *Inorganic Chemistry: Principles of Structure and Reactivity*, 3rd ed.; Harper & Row: New York, 1983; p 258.

(26) LaPlaca, S. J.; Ibers, J. A. *Inorg. Chem.* **1965**, *4*, 778.

we have been unable to grown suitable crystals for study. The $^{31}P\{^1H\}$ data for **2a** and **2b** are similar and reveal the expected AB pattern; the doublets at δ 44.3 and 33.6 ppm in **2a** and **2b**, respectively, are readily assigned to the PPh_3 ligands,[27] and the lower field doublets at 77.5 and 76.2 ppm, to the ferrocenyl phosphorus atoms.

The structure of **3**, Figure 3, reveals a hydrido- and dichloro-bridged dinuclear complex that has one η^2-H_2 ligand at one Ru and a terminal hydride ligand at the other Ru. The dihydrogen ligand bond length, H(1)–H(2), is 0.80 (6) Å, and this ligand is symmetrically coordinated, "side-on" to the Ru atom bearing the isoPFA ligand. This is one of the few reported structures to reveal an η^2-H_2 ligand and is the first crystal structure of a dinuclear dihydrogen complex.[5] Apart from **4** and **7**, other related dinuclear complexes are $(\eta^2\text{-}H_2)(PCy_3)_2Ru(\mu\text{-}H)_3RuH(PCy_3)_2$[28] and $(\eta^2\text{-}H_2)(dppb)Ru(\mu\text{-}Cl)_3RuCl(dppb)$,[29] where Cy = cyclohexyl and dppb = $Ph_2P(CH_2)_4PPh_2$. The H–H distance in **3** is similar to that found in mononuclear η^2-H_2 complexes.[29,30]

The bridging hydride is unsymmetrically coordinated: Ru(1)–H(12) = 1.71 (4) Å; Ru(2)–H(12) = 1.49 (4) Å. The Ru–(H_2) distances, Ru(1)–H(1) = 1.50 (4) Å and Ru(1)–H(2) = 1.47 (4) Å, are not significantly different from the terminal Ru(2)–H(13) distance of 1.50 (4) Å. The H–H bond is parallel to the Ru(1)–Ru(2) direction, and the plane defined by Ru(1), H(1) and H(2) roughly bisects the P(1)–Ru(1)–N and H(12)–Ru(1)–Cl(1) angles.

Except for the nitrogen atom, the skeleton of **3** is approximately superimposable on the skeletons of the analogous structures of **4**[31] and **7**,[8b,10] to the point that the bond distances and angles are remarkably similar. For example, distances for "Ru(1)–Ru(2)" are all between 2.80 and 2.83 Å, and the corresponding sets of Ru–P bond lengths are very similar: Ru(2)–P(2) = 2.226–2.230 Å, Ru(2)–P(3) = 2.249–2.281 Å, and Ru(1)–P(1) = 2.240–2.271 Å (see Figure 3). The Ru(1)–N distance of 2.300 Å in **3** may be compared with the corresponding Ru(1)–P(4) bond lengths in **4**[31] and **7**[8b] of 2.39 (1) Å. These close similarities in skeletal structures provide further support for **4** and **7** being η^2-H_2 complexes like **3**.[5,10]

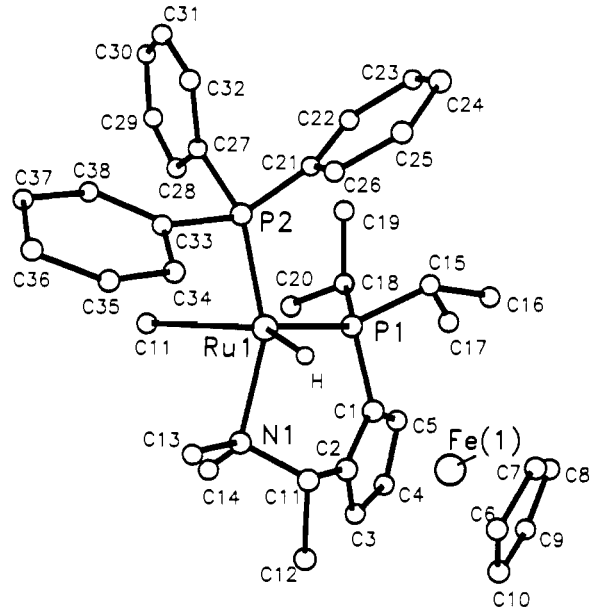

Figure 5. PLUTO plot of the structure of **5**. The possible location of the ruthenium-bound H atom is shown.

The Ru(1)–N distance, 2.300 (4) Å, in **3** is similar to that in **2b**, 2.273 (12) Å (and in **5**, 2.27 (1) Å; see below). The longest Ru–Cl distance in each of the three structures **3**, **4**, and **7** is the Ru(2)–Cl(1) bond (e.g., 2.6198 (23) Å in **3**), and this is attributed to this chloride being in a position trans to a hydride. (The ^1H NMR chemical shift of the terminal hydride for each complex (e.g., δ –18.6 for **3**) is consistent with its position trans to a ligand (Cl) of weak trans influence, and the magnitudes of the coupling constants for this resonance are in the range typical of a hydride cis to a phosphine ligand.[23]) The other Ru–μ-Cl distances in **3** (2.453 (2), 2.435 (2), and 2.528 (2) Å) and in **4** and **7** (2.435–2.48 Å) are longer than those in **2b** (average 2.39 Å). The trans influence of the η^2-H_2 ligand is weak, and consequently the shortest Ru–Cl distance in these molecules is that of Ru(1)–Cl(2) (e.g., in **3**, 2.435 (2) Å).

The unsymmetrical nature of the bridging H(12) in **3** is surprising, but can be rationalized by using electron counting; the shorter Ru(2)–H(12) distance is about the same as other Ru–H distances in the molecule. Thus, if the bridging hydride atom is considered to be coordinated solely to Ru(2), and the existence of a metal-metal bond is assumed, the electron count is 18 at each Ru atom; the Ru–Ru distance of 2.811 Å is in the range generally found for a Ru–Ru single bond (2.632–3.034 Å).[32]

The structure of **5**, $Ru(H)(Cl)(PPh_3)$(isoPFA), is shown in Figure 5, and is a rare example of a structurally characterized five-coordinate ruthenium hydride.[33] The ruthenium atom is situated in a distorted trigonal bipyramidal environment although the hydride was not unambiguously located in the refinement. However, the analytical and spectroscopic data leave no doubt that the formulation is correct. The ferrocenyl P–N ligand occupies equatorial and axial sites in the complex, subtending an angle of 98.0 (3)° at the ruthenium. The corresponding angle in **2b** is 97.0 (4)°, and in **3**, 96.5 (1)°. In all three complexes the C_5 rings are almost eclipsed. In **5**, the Ru–Cl (2.440 (3) Å) and

(27) Jessop, P. G.; Rettig, S. J.; Lee, C.-L.; James, B. R. *Inorg. Chem.* **1991**, *30*, 4617.
(28) Arliguie, T.; Chaudret, B.; Morris, R. H.; Sella, A. *Inorg. Chem.* **1988**, *27*, 598.
(29) Joshi, A. M.; James, B. R. *J. Chem. Soc., Chem. Commun.* **1989**, 1785.
(30) (a) Kubas, G. J. *Acc. Chem. Res.* **1988**, *21*, 120. (b) Henderson, R. A. *Transition Met. Chem.* **1988**, *13*, 474. (c) Crabtree, R. H.; Hamilton, D. G. *Adv. Organomet. Chem.* **1988**, *28*, 299. (d) Crabtree, R. H. *Acc. Chem. Res.* **1990**, *23*, 95. (e) Gusev, D. G.; Vymenits, A. B.; Bakhmutov, V. I. *Inorg. Chem.* **1992**, *31*, 2.
(31) The crystal analyzed grew in an NMR tube containing a toluene-d_8 solution of the bis-DMA solvate of **4** (see Experimental Section). Diffraction data were collected on an orange block using the procedures outlined for **5**. Programs used for data reduction, structure solution, and refinement are also identical to those detailed for compound **5**. Crystal data: $C_{72}H_{64}P_4Cl_2Ru_2{\cdot}C_7D_8$, fw = 1418.39, dimensions 0.52 × 0.24 × 0.10 mm, monoclinic, space group $P2_1/c$, a = 15.866 (5) Å, b = 18.931 (5) Å, c = 24.472 (7) Å, β = 108.69 (2)°, V = 6963 (3) Å^3, ρ_{calc} 1.35 g cm^3, μ = 6.37 mm^{-1}. Data collected in quadrants $h,k,\pm l$, with $4 < 2\theta < 45°$ and T = 163 K. Symmetry equivalent data were averaged to give a data set of 8996 (reflections R_{int} = 0.0234). Empirical absorption corrections were applied with transmission factors 0.859 (max) 0.796 (min). Patterson search, least squares, and Fourier syntheses revealed all atoms of the ruthenium complex together with those of a deuterotoluene of crystallization. Hydrogen atoms were input on the phenyl rings in calculated positions. Residuals following final blocked matrix refinements were R_f = 0.0780 (R_w = 0.0792) for 4507 observed reflections ($I > 2\sigma(I)$). A final Fourier synthesis revealed a number of peaks in the range 1.4–1.2 e Å^{-3}, consistent with an additional molecule in the crystal lattice, perhaps in partial occupancy (probably DMA). It was not possible to obtain a suitable resolution of this additional molecule and, in consequence, attempts to locate and refine the metal-bound H atoms were abandoned. Some selected bond lengths (Å): Ru(1)–Ru(2) 2.831 (2), Ru(2)–Cl(1) 2.476 (4), Ru(2)–Cl(2) 2.565 (5), Ru(2)–P(3) 2.251 (4), Ru(2)–P(2) 2.226 (5), Ru(1)–Cl(1) 2.435 (4), Ru(1)–Cl(2) 2.469 (4), Ru(1)–P(1) 2.281 (4), Ru(1)–P(4) 2.391 (5). The labeling corresponds to that given in Figure 3, but with N replaced by P(4). Supplementary material deposited for **4** comprises a perspective view, and Tables SVIII–SXI which list full crystal data, bond lengths and angles, positional and thermal parameters for non-H atoms and H atoms parameters.
(32) (a) Knox, S. A. R.; Macpherson, K. A.; Orpen, A. G.; Rendle, M. C. *J. Chem. Soc. Dalton Trans.* **1989**, 1807. (b) Yawney, D. B. W.; Doedens, R. J. *Inorg. Chem.* **1972**, *11*, 838. (c) Mason, R.; Thomas, K. M.; Gill, D. F.; Shaw, B. L. *J. Organomet. Chem.* **1972**, *40*, C67.
(33) Schroder, M.; Stephenson, T. A. In *Comprehensive Coordination Chemistry*; Wilkinson, G., Gillard, R. D., McCleverty, J. A., Eds.; Pergamon: Oxford, England, 1987; Vol. 4, Chapter 45, p 452.

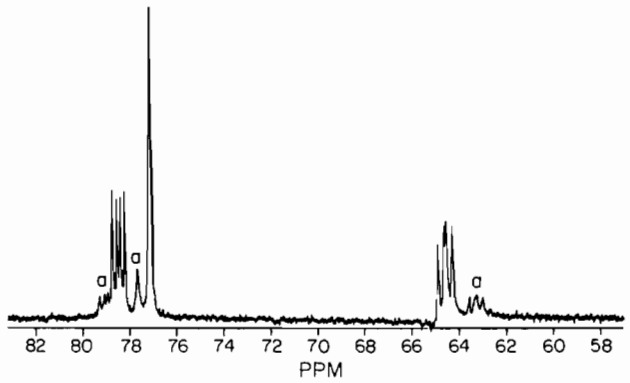

Figure 6. $^{31}P\{^1H\}$ NMR spectrum of **3**, at 121 MHz in CD_2Cl_2. Resonances marked "a" are probably due to an isomer of **3**.

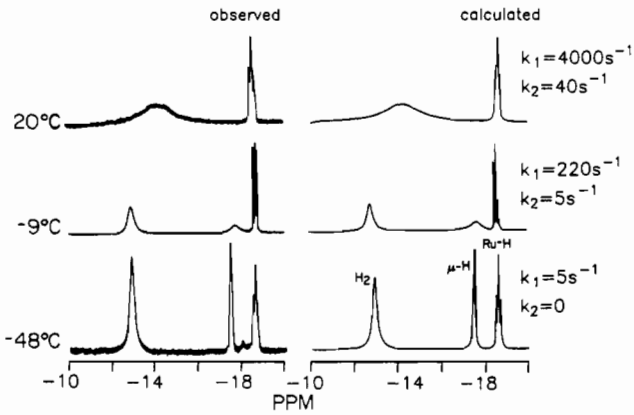

Figure 7. Observed and calculated high-field ^1H NMR spectra of **3** at 300 MHz in CD_2Cl_2.

Ru–P(2) (2.249 (3) Å) distances are unexceptional; however, Ru–P(1) (2.178 (3) Å) shows a significant shortening compared to corresponding values in **2b** (2.208 (6) Å) and **3** (2.2403 (21) Å).

NMR Studies. The $^{31}P\{^1H\}$ NMR spectrum of **3**, which is invariant with temperature, is shown in Figure 6. The two major doublet-of-doublets must be due to P(2) and P(3), which are cis to each other (J_{PP} = 40 Hz), and have differing structural relationships (and unresolved couplings) to P(1). The upfield resonance centered at δ 64.6 is assigned to the P(3) atom, which is trans to the bridging hydride, H(12), and the resonance centered at 78.5 is assigned to the P(2) atom, which is trans to a bridging chloride; the broad singlet at δ 77.2 arises from P(1) of the P–N ligand. The observed couplings[8] and the $^{31}P\{^1H\}$ NMR data for **3** are thus consistent with retention of the solid-state structure in solution. The three elements of chirality with **3** (the planar and central elements of the isoPFA ligand and the dinuclear skeleton itself) give rise to four diastereomers each with its corresponding enantiomer; each diastereomer (and accompanying enantiomer) will generate a pair of doublets in the $^{31}P\{^1H\}$ NMR spectrum. We consider that the two major doublet-of-doublets result from equal populations of two diastereomers related by an epimerization process; the presence of a similar second set of resonances of lesser intensity (labeled "a") is considered due to the presence of the other two diastereomers.

The upfield region in the 300-MHz ^1H NMR spectrum of **3** in CD_2Cl_2 at 20 °C under hydrogen is shown in Figure 7. The main features are a broad resonance associated with the dihydrogen and μ-H ligands and a doublet of doublets at δ –18.6 (arising from a terminal hydride), which is always accompanied by another minor doublet of doublets some 16 Hz further downfield. This minor signal probably results from a less abundant isomer, as noted in the $^{31}P\{^1H\}$ NMR spectrum; the additional minor signal seen at δ –18.1 (Figure 7, –48 °C spectrum) could arise from the associated μ-H, while the minor η^2-H_2 signal

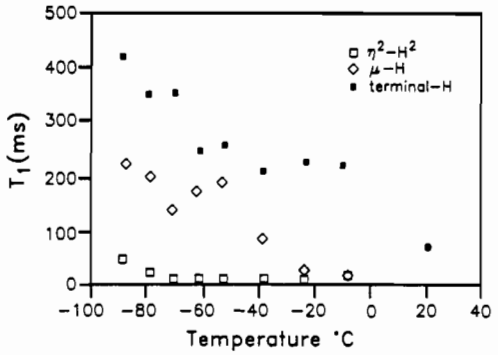

Figure 8. Variation of T_1 values with temperature for the hydrogen ligands of **3**.

is not detected. In contrast to the $^{31}P\{^1H\}$ NMR data, the ^1H NMR data reveal just one set of major and one set of minor signals. Presumably, the ^1H resonances of the two major diastereomers are experimentally indistinguishable; the same must hold for the minor diastereomers.

An exchange process occurs mainly at the isoPFA end of the dinuclear molecule, between the dihydrogen and bridging hydride ligands; the signals for these ligands are resolved, although exchange-broadened, at –9 °C, and sharpen on cooling the system to –48 °C. The upfield region at –61 °C shows δ –18.5 (t, 1H, $^2J_{PH}$ = 30 Hz, Ru–H), –17.3 (br s, 1H, μ-H), –12.8 (br s, 2H, η^2-H_2). The calculated upfield ^1H NMR spectra are also shown in Figure 7. The k_1 constant applies to the exchange process involving the η^2-H_2 and μ-H ligands while the k_2 constant applies to the exchange process involving the bridging and terminal hydride ligands. The model[34] consists of a BXYZ spin system exchanging rapidly (k_1) with an A_2XYZ spin system and slowly (k_2) with a CXYZ system, but only J_{CX} and J_{CY} were allowed to be nonzero. The T_2 values for the simulation of the η^2-H_2 ligand resonance were permitted to increase with increasing temperature, the necessary numbers being obtained by extrapolation of a log (T_2) vs (temperature, K)$^{-1}$ plot[35] from measured low-temperature values.[36] The input T_2 values for the –9 and +20 °C simulations of the other hydride resonances were given the value of 90 ms, obtained from the half-width of the terminal hydride resonance at δ –18.5 in the –9 °C spectrum; for the –48 °C simulation, values of 25 ms were used to simulate hydride peak broadening. The chemical shift of the μ-H resonance was permitted to shift slightly upfield with decreasing temperature, as found experimentally, while the shifts for the η^2-H_2 and terminal hydride ligands were taken as constant. The activation parameters for the η^2-H_2/μ-H exchange obtained from an Eyring plot of the k_1 values are $\Delta H^\ddagger$ = 52 ± 9 kJ/mol, $\Delta S^\ddagger$ = 1 ± 40 J/(mol K), and $\Delta G^\ddagger$ = 52 ± 3 kJ/mol at 20 °C.

The inversion–recovery method[37] was used to obtain T_1 measurements for the upfield resonances in the ^1H NMR spectrum of **3**; these measurements were carried out at 300 MHz, under a hydrogen atmosphere. A plot of the measured T_1 values over the range –88 to +20 °C is shown in Figure 8. The T_1 values show the presence of one η^2-H_2 ligand (e.g., at –60 °C, for the resonance at δ –12.8, T_1 = 13.8 (3) ms) and two hydrides (at –60 °C, for the resonance at δ –17.3 (μ-H) and –18.5 (terminal), the T_1 values are 182 (6) and 251 (5) ms, respectively). In general

(34) The program DNMR4 (Quantum Program Exchange No. 466) was used for the simulations. The k_1 data differ somewhat from those published in the preliminary communication,[5] because of improvements in estimates of T_2 values and chemical shift values for the fast exchange region, where these cannot be observed directly.

(35) Pople, J. A.; Schneider, W. G.; Bernstein, H. J. *High Resolution NMR*; McGraw-Hill: New York, 1959.

(36) Hampton, C. R. S. M. Ph.D. Thesis, University of British Columbia, 1989.

(37) (a) Crabtree, R. H.; Lavin, M.; Bonneviot, L. *J. Am. Chem. Soc.* **1986**, *108*, 4032. (b) Hamilton, D. G.; Crabtree, R. H. *Ibid.* **1988**, *110*, 4126. T_1 values for η^2-H_2 resonances lie in the range 4–100 ms.

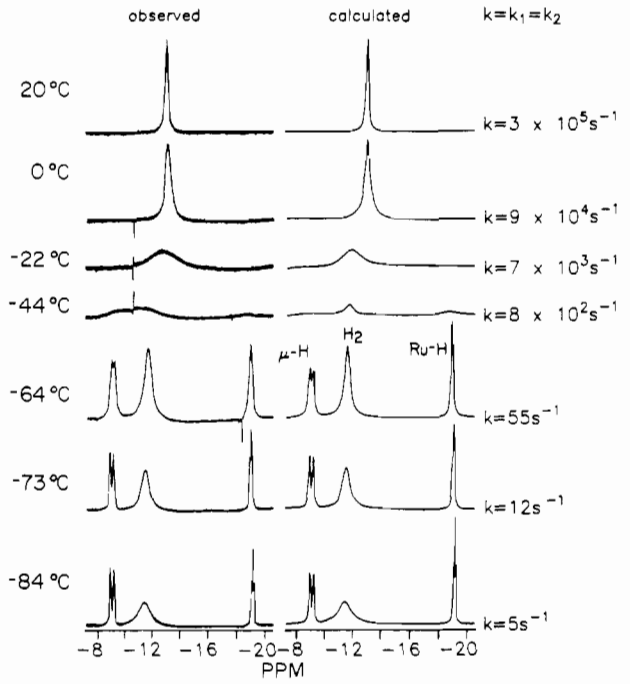

Figure 9. Observed and calculated high-field ^1H NMR spectra of **7** at 300 MHz in CD_2Cl_2.

for exchanging systems, the T_1 values begin to average when the lifetime becomes less than the T of a given state;[37] in the present case, the T_1 values of the η^2-H_2 and μ-H ligands begin to average at about –50 °C, where the exchange time (Figure 7) = $1/k_1$ = $1/(5\ s^{-1})$ = 200 ms. The T_1 value of the terminal Ru–H begins to average with those of the other hydrogen ligands at about –10 °C, and since the terminal hydride T_1 value at this temperature is 230 ms, an estimate of k_2 from the T_1 measurements would be about 4 s^{-1}; this is consistent with the estimate from the line shape simulation (Figure 7) of k_2 = 5 s^{-1} at –9 °C. The T_1 values of the resonances for the μ-H and η^2-H_2 ligands are completely averaged at –9 °C (Figure 8).

Spin-saturation transfer studies at 300 MHz, under hydrogen, revealed no spin transfer between the three upfield resonances at –48 °C; however, at –9 °C, irradiation of the η^2-H_2 resonance caused collapse of the μ-H resonance, although irradiation of the μ-H resonance decreased the η^2-H_2 resonance by only 60%. When the μ-H resonance was irradiated, there was also a reduction in the terminal Ru–H resonance peak area by ~20%, and when the terminal Ru–H was irradiated, there was approximately 50% reduction in the μ-H resonance.

Corresponding ^1H NMR measurements were made on the tri-(*p*-tolyl)phosphine complex **7**.[38] Figure 9 shows the observed and calculated spectra over the range +20 to –84 °C. The exchange model used for the simulation is similar to that employed above for **3**, but with additional couplings available, namely: $A_2 \rightleftharpoons BXYZ \rightleftharpoons CXY$, with $k = k_1 = k_2$, defined as before. The proton B (μ-H), with a long T_2, exchanges with both the A protons (η^2-H_2), which have short T_2 values, and also with proton C (terminal-H), which has a long T_2 value. The low-field resonance is due to **B**, the high-field resonance to C, and the intermediate resonance to A_2. The coupling constants used in the simulation are as follows: J_{BX}, J_{BY}, and J_{BZ} (78, 8, and 2 Hz, respectively) and J_{CX}, J_{CY} (both 27 Hz); these J values agree with those quoted previously.[8,10] Values of shifts obtained from the slow exchange spectra were plotted against temperature and extrapolated to give the higher temperature numbers. The T_2 values used for the terminal and bridging hydride were obtained from the half-widths of resonances in the low-temperature spectra, and were held

(38) Some NMR spectra of **7** have been described previously.[8,10]

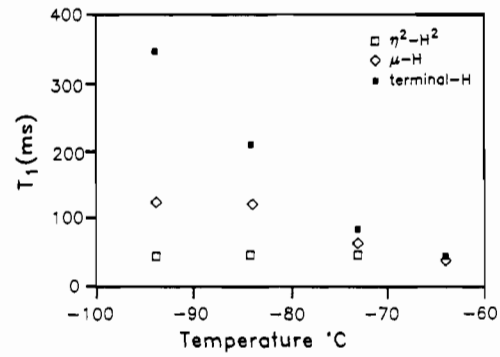

Figure 10. Variation of T_1 values with temperature for the hydrogen ligands of **7**.

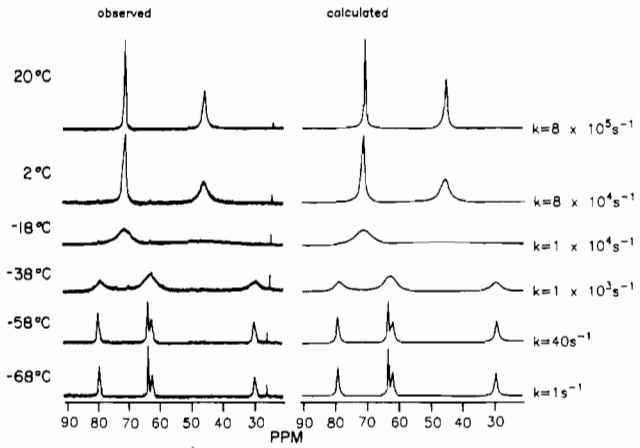

Figure 11. Observed and calculated $^{31}P\{^1H\}$ NMR spectra of **4** at 121 MHz in toluene-d_8.

constant, at 20 ms, over the temperature range of the simulation; however, the T_2 of the dihydrogen ligand was varied as described above for **3**. Activation parameters obtained from an Eyring plot of the exchange constants are $\Delta H^\ddagger$ = 49 ± 7 kJ/mol, $\Delta S^\ddagger$ = 30 ± 30 J/(mol K), and $\Delta G^\ddagger$ (20 °C) = 41 ± 2 kJ/mol. Values of T_1 measured over the temperature range –94 to –64 °C are displayed in Figure 10. At –94 °C, T_1 (ms) values are 44 (η^2-H_2), 120 (μ-H), and 350 (terminal H).

The $^{31}P\{^1H\}$-NMR spectra of the bis-DMA solvate of **4** exhibited the same features as the solvate-free complex generated in situ under H_2 from $[RuCl_2(PPh_3)_2]_2$ and Proton Sponge, Figure 11. Peaks at δ 70.5 and 46.0 ppm at ambient temperature broaden on cooling to give four resolved resonances at –58 °C, whose chemical shifts (79.5 (s), 63.5 (s), 62.5 (s), 29.5 (s)) remain temperature-invariant down to –88 °C; thus there is rapid exchange of phosphorus environments at ambient temperature. The calculated and observed $^{31}P\{^1H\}$ NMR spectra are shown. No couplings are resolved at 121 MHz, but the variation in broadness of these peaks (at –68 °C, $w_{1/2}$ = 78, 47, 94, and 100 Hz, respectively) is consistent with the values of coupling constants reported by Dekleva et al.[8] for the 32.4-MHz spectrum. The model used for the simulation was an ABCD ⇌ BADC exchange system, defined by a first-order rate constant, k. The T_2 values were calculated from the peak half-widths at –68 °C, and T_2 values and chemical shifts were kept constant over the temperature range of the simulation. (These T_2 values are merely input to a computer program for simulation purposes and probably reflect values of coupling constants more than actual T_2 values.) The exchange constants, also shown in Figure 11, indicate rapid exchange at 20 °C ($k = 8 \times 10^5\ s^{-1}$). An Eyring plot yields values for $\Delta H^\ddagger$ (70 ± 12 kJ/mol), $\Delta S^\ddagger$ (110 ± 50 J/(mol K)), and $\Delta G^\ddagger$ (38 ± 3 kJ/mol at 20 °C) for the phosphine exchange. Errors in k values from these line-shape analyses are greater for faster and slower exchange, because line shapes change less with

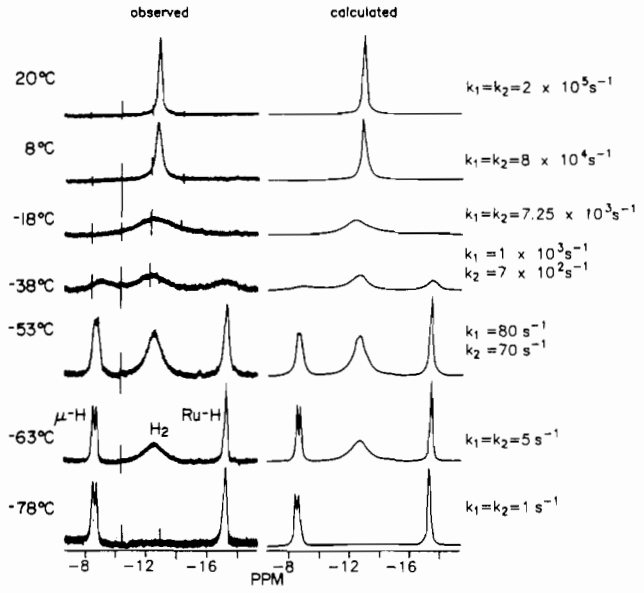

Figure 12. Observed and calculated ^{1}H NMR spectra of **4**.

temperature (and therefore the k values) in these regimes, and the errors in these k values could be 50%.

The ^{1}H NMR spectrum of **4** at 20 °C (Figure 12) shows a signal at −12.9 ppm ($w_{1/2}$ = 75 Hz) that broadens on cooling to −18 °C, while further cooling yields the slow-exchange spectra; e.g. at −69 °C: δ −8.6 (d, 1 μ-H, $^2J_{PH}$ = 66 Hz), −12.6 (br s, $w_{1/2}$ ~500 Hz, 2 η^2-H_2 protons), −17.2 (t, 1 terminal H, $^2J_{PH}$ = 30 Hz). Exchange-spectra simulations thus employed an $A_2 \rightleftharpoons BX \rightleftharpoons CXY$ exchange model corresponding to that used for **7**, but only a single coupling constant is resolved for the B(μ-H) proton. The exchange constant for the $A_2 \rightleftharpoons BX$ exchange is again k_1, and for the $BX \rightleftharpoons CXY$ process is k_2. Chemical shift data at lower temperatures were again extrapolated to give values at higher temperatures, although the shift of the η^2-H_2 resonance was held invariant with temperature as line broadening above and below −53 °C made observation of any change of chemical shift with temperature difficult. The T_2 values used for the bridging and terminal hydrides were 8 and 12 ms, respectively, for all simulations except for the one for the spectrum at −78 °C, where slightly lower values (6 and 8 ms, respectively) were used in order to mimic broadening possibly caused by limitations in solubility at this temperature. T_2 for the η^2-H_2 resonance was again allowed to increase with increasing temperature, as described for **3** and **7**, but using only data above about −55 °C. The exchange constants shown in Figure 12 quantify the rate of exchange at various temperatures. As with **7**, this rate is rapid at ambient temperature (at 20 °C, $k_1 = k_2 = 2 \times 10^5$ s^{-1}) and slows as the temperature is lowered (at −78 °C, $k_1 = k_2 = 1$ s^{-1}): the constants, k_1 and k_2, are the same within experimental error. An Eyring plot for either rate constant yields values for $\Delta H^\ddagger$, $\Delta S^\ddagger$, and $\Delta G^\ddagger$ (20 °C) of 60 ± 10 kJ/mol, 60 ± 40 J/(mol K), and 41 ± 2 kJ/mol, respectively.

The quality of the spectra of **4** used for low-temperature T_1 measurements was poor because of the dilute solutions used, and errors in T_1 values may be as high as 20%. Figure 13 shows the variation of T_1 values with temperature. As in the plots of Figures 8 and 10, a minimum T_1 cannot be located because of the exchange processes, and attempts to calculate H–H distances from the T_1 data would be of little value.[39] The T_1 values completely average at temperatures above ~−40 °C. However, the T_1 values (ms) at −73 °C (300 at δ −8.6, 77 at δ −12.6, 900 at δ −17.2) confirm the presence of an η^2-H_2 resonance at −12.6 ppm. From −40 °C

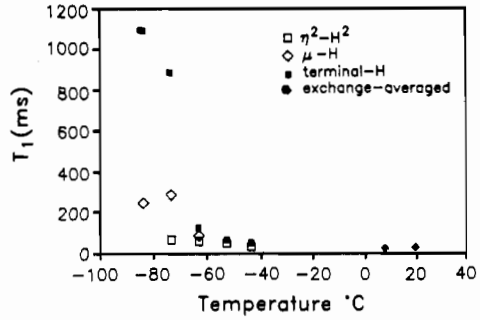

Figure 13. Variation of T_1 values with temperatures for the hydride ligands of **4**.

up to room temperature, the averaged T_1 value shows little change, with values of 40 ms at −40 °C and 20 ms at both 6 and 20 °C.

The model (P(1) exchanging with P(2), P(3) exchanging with P(4)) that successfully simulates the exchange process observed in the ^{31}P spectrum of complex **4** probably reflects the change in phosphorus environments caused by the hydrogen ligand exchange processes. Thus, for example, P(1) on Ru(1) and P(2) on Ru(2) exchange environments as the η^2-H_2 ligand resides on alternate ruthenium centers. This rationalizing of the variable-temperature ^{31}P behavior requires the exchange rate constants from the ^{31}P and ^{1}H NMR simulations to be equal within experimental error, and this is probably true: the rate constant for the phosphorus exchange at 20 °C ($k = 8 \times 10^5$ s^{-1}) and that of the hydrogen exchange at 20 °C ($k = 2 \times 10^5$ s^{-1}) are in reasonable agreement, considering the error estimate of ±50% given above for k values in the fast-exchange region.

The ^{1}H NMR exchange rate constants for hydrogen ligand exchange for the two analogues **4** and **7** are similar. However, comparison of the ^{1}H NMR spectra of **4** at −63 °C and **7** at −64 °C reveals slightly more broadening of signals for the latter even though resolution is better because of the higher solubility of this complex.

The mechanism of exchange may involve coordinated η^3-H_3 units and/or bridging dihydrogen. Involvement of an η^3-H_3 unit in hydride/dihydrogen exchange in $[Ir(H)(\eta^2\text{-}H_2)(bq)(PPh_3)_2]^+$ (bq = 7,8-benzoquinolate) has been suggested.[37] Evidence for the existence of the trihydride ligand, for example, in the complexes $[Ir(H_3)Cp(L)]^+$ (Cp = η^5-C_5H_5; L = PMe_3, PPh_3, $AsPh_3$),[40] $MH_3Cp'_2$ (where M = Nb, Ta; Cp′ = C_5H_4Me, $C_5H_4(SiMe_3)$ or $C_5H_3(SiMe_3)_2$),[41] and $RuH_3(C_5Me_5)(PCy_3)$[41b] has recently been refuted.[42] There is no precedent for bridging H_2; a complex $CpRu(\mu\text{-}H)_4RuCp$ was initially thought to possibly have two bridging H_2 molecules,[43] but a reinterpretation of the X-ray crystallographic data later showed that all the bridging hydrides are, in fact, classical.[44] That hydrogen ligands can interconvert from classical hydrides to a nonclassical dihydrogen ligand in solution is now well documented.[30,45] Species with polyhydrogen chains have also been invoked as possible exchange intermediates.[46]

To our knowledge, the activation parameters for the hydrogen exchange processes within **3**, **4**, and **7** are the first reported for dinuclear η^2-H_2 complexes. The exchange in **4** and **7** involving

(39) Bautista, M.; Earl, K. A.; Morris, R. H.; Sella, A. *J. Am. Chem. Soc.* **1987**, *109*, 3780.

(40) Heinekey, D. M.; Payne, N. G.; Schulte, G. K. *J. Am. Chem. Soc.* **1988**, *110*, 2303.

(41) (a) Antinolo, A.; Chaudret, B.; Commenges, G.; Fajardo, M.; Jalon, F.; Morris, R. H.; Otero, A.; Schwetzer, C. T. *J. Chem. Soc., Chem. Commun.* **1988**, 1210. (b) Chaudret, B.; Commenges, G.; Jalon, F.; Otero, A. *J. Chem. Soc., Chem. Commun.* **1989**, 210.

(42) Heinekey, D. M. *J. Am. Chem. Soc.* **1991**, *113*, 6074 and references therein.

(43) Suzuki, H.; Omori, H.; Lee, D. H.; Yoshida, Y.; Moro-oka, Y. *Proc. 6th Int. Symp. Homog. Catal* 1988, P-115.

(44) Marsh, R. E. *Organometallics* **1989**, *8*, 1583.

(45) For example: (a) Howard, M. T.; George, M. W.; Hamley, P.; Poliakoff, M. *J. Chem. Soc., Chem. Commun.* **1991**, 1101. (b) Kubas, G. J.; Unkefer, C. J.; Swanson, B. I.; Fukushima, E. *J. Am. Chem. Soc.* **1986**, *108*, 7000.

(46) Pacchioni, G. *J. Am. Chem. Soc.* **1990**, *112*, 80.

the η^2-H_2 ligand is faster than that in **3** by a factor of at least 50 and involves all the hydrogen ligands, in contrast to the behavior of **3** where the terminal hydride ligand is involved only in a much slower exchange process. (In **3**, this latter exchange is about 100 times slower than that existing between the μ-H and η^2-H_2 at the Ru center chelated by the P–N ligand.) The exchange in **4** and **7** is easily pictured within an intramolecular process (without considering the nature of the intermediates) in which one hydrogen of the η^2-H_2 at Ru(1) displaces the bridged hydride, which itself then reforms an η^2-H_2 at Ru(2) with the initially terminal hydride. In **3**, because of the P–N ligand at Ru(1) and the two monodentate PR_3 ligands at Ru(2), the same picture leads to formation of an isomer with the η^2-H_2 at Ru(2) and the terminal hydride at Ru(1); an overall exchange process requires a corresponding reverse process with a further activation energy. The data imply that an η^2-H_2 ligand exchanges with a bridged hydride much more readily than does a terminal hydride, and this seems reasonable in terms of the possible intermediates suggested above. Within **3**, using the k_2 data at just two temperatures (+20 and −9 °C; see Figure 7), which gives $\Delta H^{\ddagger} \sim 45$ kJ/mol and $\Delta S^{\ddagger} \sim -65$ J/(mol K), the slower exchange with the terminal hydride (vs. the k_1 process) results from a more unfavorable entropy of activation.

Hydrogen-exchange processes within $M(H_2)H(PPh_2(CH_2)_2PPh_2)_2^+$ species (M = Fe, Ru)[47] occur with $\Delta G^{\ddagger}$ values at 20–25 °C of ~60 kJ/mol, some 10–20 kJ/mol higher than those noted here for the η^2-H_2/μ-H exchange. Conversion from an η^2-H_2 ligand to a classical dihydride and the reverse process, at a single Ru center within cyclopentadiene/chelating ditertiary phosphine systems [$Ru^{IV}(H)_2 \rightleftharpoons Ru^{II}(\eta^2\text{-}H_2)$], both require $\Delta G^{\ddagger}$ values (20–25 °C) of ~80 kJ/mol,[24c] and it is not necessary to invoke such an equilibrium in the present work to account for the observed exchange processes.

The suggestion has been made[39,48] that an N_2 ligand should be replaceable by an η^2-H_2 ligand when the dinitrogen stretching frequency falls in the range 2060–2150 cm^{-1}. Examples of replacement of coordinated dihydrogen by dinitrogen have also been observed;[29,37,39] one of these systems involves the (L)(dppb)Ru(μ-Cl)$_3$RuCl(dppb) species (L = η^2-H_2 or σ-N_2), where in fact ν_{N_2} is 2175 cm^{-1} (in CH_2Cl_2).[29] However, complexes **4** and **7** do not seem to react with nitrogen, and their decomposition, which occurs slowly in the absence of hydrogen, was not appreciably affected by the presence of dinitrogen.

Acknowledgment. The authors thank the Natural Sciences and Engineering Research Council of Canada for financial assistance, Johnson Matthey for the loan of $RuCl_3 \cdot 3H_2O$, and Dr. Ward T. Robinson, University of Canterbury, New Zealand, for X-ray data collections of compounds **4** and **5**.

Supplementary Material Available: Table SI, giving full crystal data for **2b** and **5**, Tables SII–SVII, listing for **2b** and **5**, respectively, anisotropic thermal parameters, H-atom parameters, and all bond lengths and angles, Tables SVIII–SXI, listing crystallographic data for **4** (see ref 31), and Figure SI, showing a perspective view of complex **4** (22 pages). Ordering information is given on any current masthead page.

(47) Morris, R. H.; Sawyer, J. F.; Shiralian, M.; Zubkowski, J. D. *J. Am. Chem. Soc.* **1985**, *107*, 5581.

(48) Morris, R. H.; Earl, K. A.; Luck, R. L.; Lazarowych, N. J.; Sella, A. *Inorg. Chem.* **1987**, *26*, 2674.